JOC The Journal of Organic Chemistry

Article

pubs.acs.org/joc

Oligonucleotides with "Clickable" Sugar Residues: Synthesis, Duplex Stability, and Terminal versus Central Interstrand Cross-Linking of 2′-O-Propargylated 2-Aminoadenosine with a Bifunctional Azide

Suresh S. Pujari,[†,‡] Peter Leonard,[†] and Frank Seela*[,†,‡]

[†]Laboratory of Bioorganic Chemistry and Chemical Biology, Center for Nanotechnology, Heisenbergstraße 11, 48149 Münster, Germany

[‡]Laboratorium für Organische und Bioorganische Chemie, Institut für Chemie neuer Materialien, Universität Osnabrück, Barbarastraße 7, 49069 Osnabrück, Germany

Supporting Information

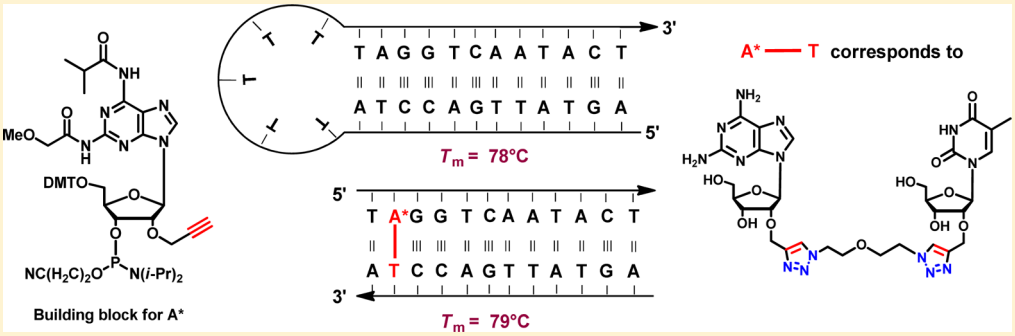

ABSTRACT: Duplex DNA with terminal and internal sugar cross-links were synthesized by the CuAAC reaction from oligonucleotides containing 2′-*O*-propargyl-2-aminoadenosine as a clickable site and a bifunctional azide (**4**). Stepwise click chemistry was employed to introduce cross-links at internal and terminal positions. Copper turnings were used as catalyst, reducing the copper load of the reaction mixture and avoiding complexing agents. For oligonucleotide building block synthesis, a protecting group strategy was developed for 2′-*O*-propargyl-2-aminoadenosine owing to the rather different reactivities of the two amino groups. Phosphoramidites were synthesized bearing clickable 2′-*O*-propargyl residues (**14** and **18**) as well as a 2′-deoxyribofuranosyl residue (**10**). Hybridization experiments of non-cross-linked oligonucleotides with 2,6-diaminopurine as nucleobase showed no significant thermal stability changes over those containing adenine. Surprisingly, an isobutyryl group protecting the 2-amino function has no negative impact on the stability of DNA−DNA and DNA−RNA duplexes. Oligonucleotide duplexes with cross-linked 2′-O-propargylated 2-aminoadenosine (**1**) and 2′-O-propargylated adenosine (**3**) at terminal positions are significantly stabilized (ΔT_m = +29 °C). The stability results from a molecularity change from duplex to hairpin melting and is influenced by the ligation position. Terminal ligation led to higher melting duplexes than corresponding hairpins, while duplexes with central ligation sites were less stable.

INTRODUCTION

The stabilization of nucleic acids assemblies (duplexes, triplexes, and other supramolecular structures) plays a crucial role in chemical and biochemical applications of DNA or RNA and for the construction of nanoscopic devices in material science.[1] Stable supramolecular assemblies of DNA find use in the arrangement of nanostructures by which DNA machines such as DNA tweezers, walkers, and steppers are formed.[2] Antisense therapeutics were stabilized by backbone modification or replacement of canonical bases by modified nucleosides.[3] Such second-generation synthetic oligonucleotides having 2′-O-modifications are promising candidates in antisense technology (e.g., for the selective silencing of certain genes).[4]

Another way to strengthen the duplex structure is to introduce cross-links in DNA or RNA. The origin of cancer chemotherapy goes back to the toxic action of nitrogen mustard acting as a bifunctional DNA cross-linker. Platinum(II) compounds are used in cancer treatment for cross-linking DNA.[5] Metals such as copper, mercury, or silver ions can be considered as cross-linking reagents as they replace the canonical Watson−Crick base pairs with more stable metal base pairs.[6] Now, the Cu(I)-catalyzed azide−alkyne Huisgen−Meldal−Sharpless cycloaddition (CuAAC) "click chemistry" has emerged as a promising candidate for cross-linking because of its bioorthogonal nature and robustness of the formed triazole.[7] Our laboratory has cross-linked alkynylated DNA or RNA with bifunctional azides in a one-step process (bis-click) or in a stepwise procedure (stepwise click).[8]

Received: February 18, 2014
Published: April 2, 2014

   dx.doi.org/10.1021/jo500392j | J. Org. Chem. 2014, 79, 4423−4437

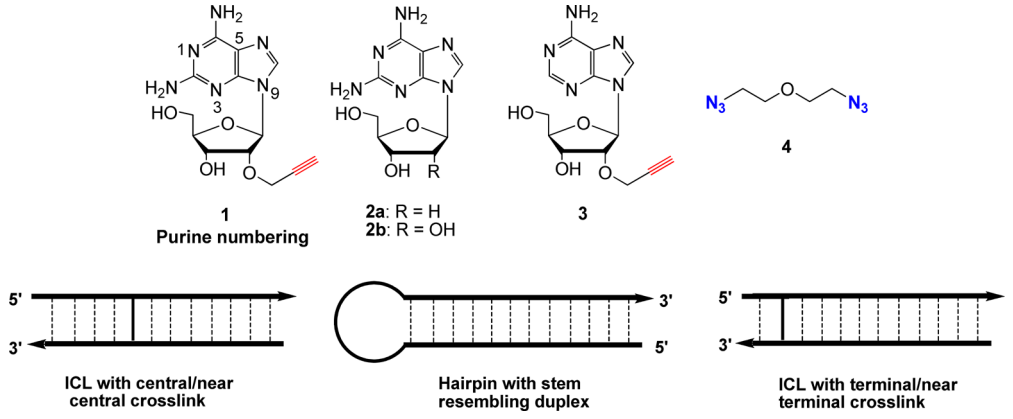

Figure 1. (Top) Sugar propargylated nucleosides and bis-azide. (Bottom) Comparison of cross-linked and hairpin DNA.

Recently, our laboratory reported on the synthesis of 2′-O-propargylated isoguanosine and on a significantly improved synthesis of 2′-O-propargylated cytidine. It was found that propargyl residues with clickable triple bonds introduced in the sugar residue of nucleosides cause only a minor change on the stability of duplexes since these units presumably lie outside the helix. Parallel stranded cross-linked oligonucleotides were also constructed using bifunctional azides.[9]

Among the various DNA and RNA constituents, the 2-amino-adenine nucleosides **2a** and **2b**, which can be used as an analogue of adenine, play a special role as stabilizing nucleosides as the base eventually forms a third hydrogen bond with dT (Figure 1).[10] Related base modified nucleosides with a pyrrolo[2,3-*d*]pyrimidine or a pyrazolo[3,4-*d*]pyrimidine skeleton have also been studied, and halogenated derivatives were used to adjust the dA−dT base pair stability to that of a dG−dC pair.[11]

This study reports on the synthesis of 2′-O-propargylated 2-aminoadenosine (**1**), the selection of suitable protecting groups for the two amino functionalities showing rather different reactivity, and the conversion into phosphoramidite building blocks. The installation of a clickable propargyl functionality in the sugar residue in combination with an additional 2-amino group into the adenine moiety is expected to stabilize duplexes over those containing only 2′-O-propargylated adenosine (**3**). Propargylated oligonucleotides were cross-linked with the bifunctional azide **4**[12] by a stepwise protocol. By this means, terminal and internal cross-links were introduced in duplexes at various positions in a site-specific way. Then, the thermal stability of ligated and nonligated duplexes is compared. As the stepwise click approach is flexible with respect to incorporation sites and cross-links, propargylated oligonucleotides were cross-linked at the center and the terminus of a duplex. Hairpins of similar structure were synthesized to compare their thermal stability to the melting of cross-linked duplexes (Figure 1).

RESULTS AND DISCUSSION

1. Synthesis and Characterization of Phosphoramidite Building Blocks. Earlier, the synthesis of 2′-*O*-propargylisoguanosine and 3′-*O*-propargylisoguanosine from the corresponding 2′-O- and 3′-O-propargylated 2-aminoadenosine precursors **1** and **6** was reported.[9] However, the yield for the propargylation of 2-aminoadenosine (**2b**) was low, and the reaction time was rather long. Therefore, an alternative route for the propargylation was explored. Compound **5**, which was synthesized according to the literature,[13a] was propargylated using NaH and propargyl bromide with tetrabutylammonium iodide as a phase transfer catalyst.[13b] Side-product formation (e.g., cleavage of the silyl clamp) was suppressed by introducing TBAF/THF into the mixture when the starting material was completely consumed (~20 min, TLC-monitoring). By this, the propargylated isomer **1** was obtained as a main product in 66% yield together with a small amount of the 3′-O-isomer **6** (8%) (Scheme 1; for details, see Experimental Section). The

Scheme 1. Propargylation of 2-Aminoadenosine 2b[a]

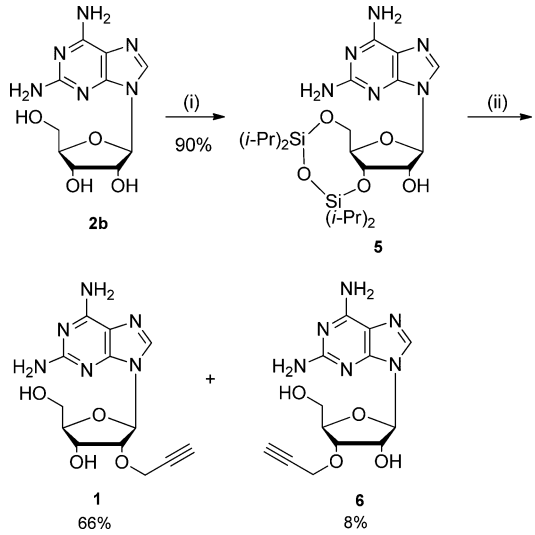

[a]Reagents and conditions: (i) $(i\text{-Pr})_2ClSiOSi(i\text{-Pr})_2Cl$, pyridine, rt, 12 h; (ii) (a) propargyl bromide, NaH, TBAI, DMF, 5−55 °C, 20 min; (b) 1 M TBAF in THF, rt, 1 h, 73%.

position of propargylation was determined by NMR spectroscopy—disappearance of the OH group in the ^1H NMR spectrum and a strong downfield shift of C-2′ in the ^{13}C NMR spectrum. The yield for the propargylated nucleoside **1** was significantly improved, from 32% to 59%, based on 2-aminoadenosine (**2b**) as a starting material (2 steps).[9]

As many contradictory reports on the protection of the two amino groups exist,[14] a protecting group strategy has to be developed for the propargylated 2-aminoadenosine phosphoramidite building block. Initially, the simultaneous protection of both amino groups with dibutylaminomethylidene residues as described for diamino pyrazolo[3,4-*d*]pyrimidine nucleosides was investigated.[14] In the case of 2′-O-propargylated compound **1**, we obtained the monoprotected (6-position) compound **7** as the

dx.doi.org/10.1021/jo500392j | J. Org. Chem. 2014, 79, 4423−4437

Scheme 2. Amidine Protection of 2′-*O*-Propargyl-2-aminoadenosine[a]

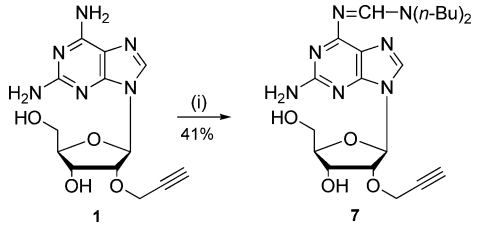

[a]Reagents and conditions: (i) *N*,*N*-dibutylformamide dimethylacetal, MeOH, 40 °C.

main product (Scheme 2) accompanied by several side products, although complete consumption of the staring material was indicated by TLC.

To shed more light on this matter and to obtain a suitable building block for oligonucleotide synthesis (see section 3), the protection of 2-amino-2′-deoxyadenosine (**2a**) was investigated. Although, the formation of new reaction products was detected by TLC during butylamidine protection, they were too labile to be isolated as clean material. Similar results have been reported for formamidine protected 2-amino-2′-deoxyadenosine.[14a] Therefore, isobutyrylation using "transient protection" conditions was studied next. In this case, diisobutyrylated compound **8** was obtained in 62% yield.[14f] 4,4′-Dimethoxytritylation of the 5′-OH group (→ **9**, 58%) and phosphitylation of the 3′-OH group gave **10** in 73% yield (Scheme 3).

Scheme 3. Synthesis of 2-Amino-2′-deoxyadenosine Phosphoramidite 10[a]

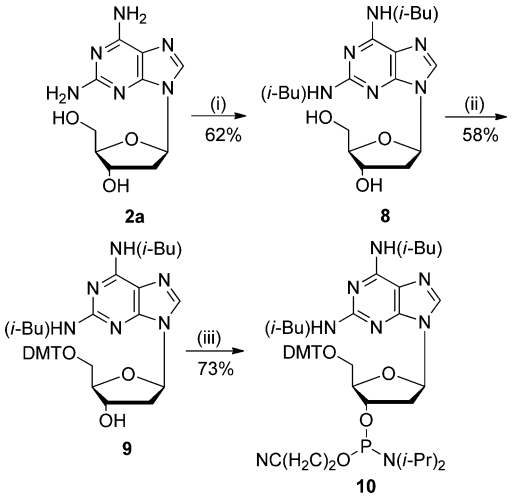

[a]Reagents and conditions: (i) *i*-BuCl, trimethylsilyl chloride, pyridine; (ii) 4,4′-dimethoxytrityl chloride, pyridine, rt; (iii) $NC(CH_2)_2OP(Cl)N(i\text{-}Pr)_2$, DIPEA, DCM, rt.

Accordingly, isobutyryl protection was performed on the 2′-O-propargylated nucleoside **1**. Surprisingly, an inseparable mixture of products was obtained. As the behavior of the propargylated nucleoside **1** was different from **2a** during isobutyryl protection, their pK_a values were determined. Both compounds showed similar pK_a values, 4.2 for **1** and 4.3 for **2a**, and they are close to that of 2-aminoadenosine **2b** (pK_a = 4.4). Therefore, we anticipated that side reactions occurring during isobutyrylation are evoked by the propargyl residue and not by the nucleobase. Thus, we went back to a stepwise protection protocol using two different amino protecting groups. At first, nucleoside **1** was selectively protected at the 2-amino group with an isobutyryl residue (→ **11**, 65%) followed by protection of the 6-amino group by a butylamidine moiety (→ **12**, 80%; Scheme 4). 4,4′-Dimethoxytritylation (→ **13**, 57%) and phosphitylation gave phosphoramidite **14** (76%).

Scheme 4. Synthesis of 2′-*O*-Propargyl-2-aminoadenosine Phosphoramidite 14[a]

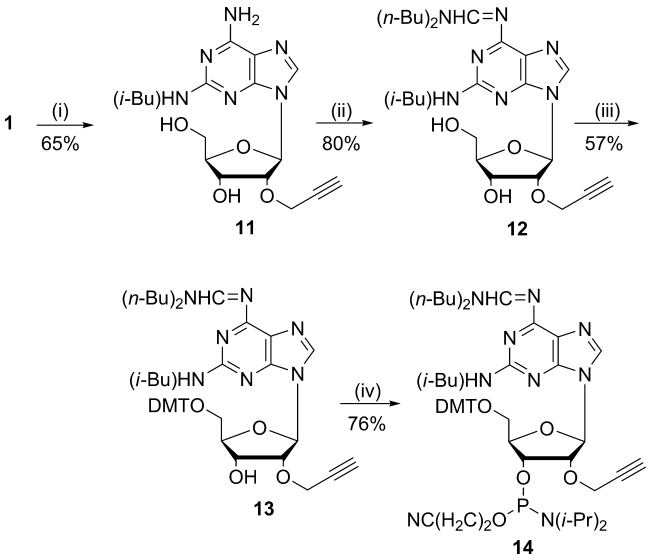

[a]Reagents and conditions: (i) *i*-BuCl, TMSCl, pyridine (−20 °C); (ii) *N*,*N*-dibutylformamide dimethylacetal, MeOH, rt; (iii) 4,4′-dimethoxytrityl chloride, pyridine, rt; (iv) $NC(CH_2)_2OP(Cl)N(i\text{-}Pr)_2$, DIPEA, DCM, rt.

Later, during oligonucleotide synthesis, we recognized that cleavage of the isobutyryl residue from the 2-amino group caused difficulties. Thus, the more labile methoxyacetyl group was introduced, which has been successfully employed for other 2-aminoadenosine derivatives.[14c] For this, nucleoside **1** was protected on the 2-amino group with the methoxyacetyl residue (→ **15**, 72%) followed by protection (isobutyryl) of the 6-amino group (→ **16**, 52%) (Scheme 5). 4,4′-Dimethoxytritylation (→ **17**, 54%) and, finally, phosphitylation afforded **18** in 74% yield (Scheme 5).

From these experiments, it is obvious that the reactivity of the two amino groups of propargylated 2-aminoadenosine (**1**) is rather different. So, a special combination of protecting groups is required composed of labile protection for the 2-amino group and a protecting group for the 6-amino group, which is more stable than that for adenosine. Taken together, the combination of the methoxyacetyl residue (2-amino) and an isobutyryl group (6-amino) represents a suitable combination to design a 2′-O-propargylated 2-aminoadenosine building block for oligonucleotide synthesis. However, base modified 2-aminoadenosine derivatives (pyrazolo[3,4-*d*]pyrimidine or pyrrolo[2,3-*d*]pyrimidine analogues) require other protecting groups as the other heterocylic skeleton changes the reactivity of the amino groups.[14]

2. Cross-Linking Performed on the 2′-O-Propargylated 2-Aminoadenosine Nucleoside 1. Earlier, it was reported that both the stepwise click and the bis-click protocol can be performed when identical nucleosides are clicked together, while a stepwise click reaction is required when the

dx.doi.org/10.1021/jo500392j | J. Org. Chem. 2014, 79, 4423−4437

Scheme 5. Synthesis of 2′-*O*-Propargyl-2-aminoadenosine Phosphoramidite 18[a]

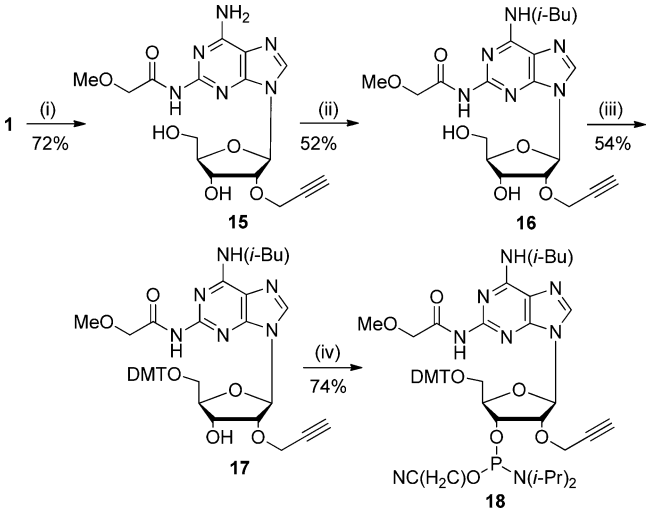

[a]Reagents and conditions: (i) trimethylsilyl chloride, methoxyacetyl chloride, pyridine, 4 °C to rt; (ii) trimethylsilyl chloride, *i*-BuCl, pyridine, 4 °C to rt; (iii) 4,4′-dimethoxytrityl chloride, pyridine, rt; (iv) $NC(CH_2)_2OP(Cl)N(i\text{-}Pr)_2$, DIPEA, DCM, rt.

nucleosides are different.[15] Once we had 2′-*O*-propargylated nucleoside **1** in hand, we studied the "click reaction" with nucleoside **1** and bis-azide **4**. First, the stepwise click functionalization of nucleoside **1** was performed with copper turnings and a 5-fold excess of bis-azide **4** furnishing the monofunctionalized nucleoside **19** in 45% yield. In the next step, **19** was converted to the cross-linked adduct **20** (42%). Alternatively, nucleoside **1** was reacted with bis-azide **4** using a nucleoside to bis-azide ratio of 2:1, affording the cross-linked adduct **20** in 60% yield (Scheme 6) (for details, see

Scheme 6. Cu(I)-Catalyzed Stepwise Click and Bis-Click Reaction Performed with Nucleoside 1 and Bis-azide 4[a]

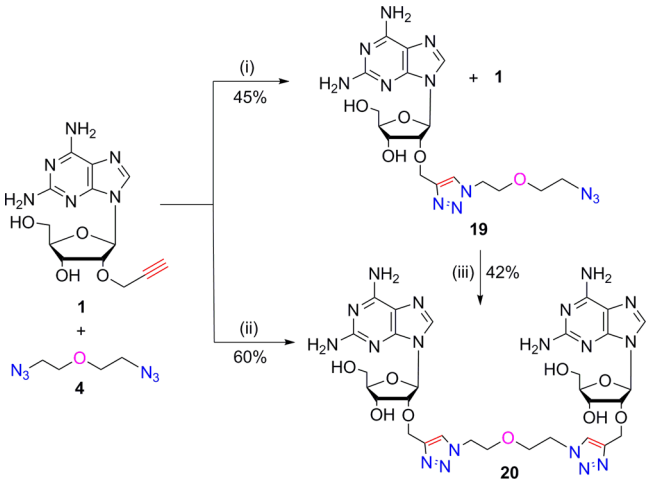

[a]Reagents and conditions: (i) copper turnings, H_2O/CH_3CN, 10:1, ratio **1**/**4** 1:5; (ii) copper turnings, H_2O/CH_3CN, 10:1, ratio **1**/**4** 2:1; (iii) copper turnings, H_2O/CH_3CN, 10:1, ratio **1**/**19** 1:1.

Experimental Section). All synthesized compounds were characterized by ^1H NMR, ^{13}C NMR, and mass spectra. DEPT-135 and $^1H-^{13}C$ gated-decoupled NMR spectra were used to assign the ^{13}C NMR signals (for details, see Experimental Section, Table 5; Supporting Information, Table S1).

3. Synthesis and Thermal Stability of DNA Duplexes and DNA−RNA Hybrids Containing 2′-O-Propargylated 2-Aminoadenosine (1). The syntheses of the propargylated phosphoramidites of canonical purine and pyrimdine nucleosides (Figure 2) have been already reported.[16,17] The 2′-*O*-propargylated

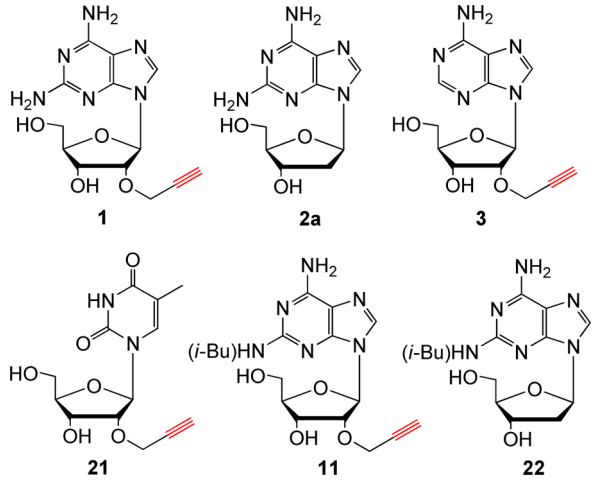

Figure 2. Structures of nucleosides used for hybridization studies on DNA duplex formation.

2-aminoadenosine phosphoramidites **14** and **18**, as well as the corresponding 2′-deoxy building block **10**, are described in this work. These building blocks, together with those of canonical nucleosides and the phosphoramidite of 1,3-propanediol[18], were used in the solid-phase synthesis of oligonucleotides. The coupling yields were always higher than 95%. Modified nucleosides were incorporated in both strands of the 12-mer DNA oligonucleotides 5′-d(TAG GTC AAT ACT) (**25**) and 3′-d(ATC CAG TTA TGA) (**26**), which served as reference duplex. The duplex stability of oligonucleotides incorporating 2′-O-propargylated 2-aminoadenosine **1** is compared with that of oligonucleotides containing 2′-O-propargylated adenosine (**3**) or the nonpropargylated nucleoside 2-amino-2′-deoxyadenosine (**2a**). The removal of the isobutyryl residue from the 2-amino group of compounds **2a** and **1** was encountered with difficulties during oligonucleotide synthesis, as this group withstands standard deprotection conditions. However, it could be cleaved under harsh conditions ($MeNH_2$/aq NH_3, 1:1, 60 °C, 1 h). In contrast, the methoxyacetyl group in the 2-position was easily removed. Thus, a skillful choice of building blocks in combination with the deprotection conditions made oligonucleotides with or without isobutyryl residue easily accessible. All oligonucleotides were characterized by MALDI-TOF mass spectrometry (Table 1). Both the protected and nonprotected oligonucleotides were used for hydridization studies (Table 2; Experimental Section).

Earlier hybridization studies with canonical ribonucleosides bearing 2′-O-propargyl residues were performed by Sproat and co-workers. In their studies, thermal and enzymatic duplex stabilization of the propargyl modification was compared to 2′-*O*-methyl or 2′-*O*-methoxyethyl derivatives, and a possible application in antisense oligonucleotides was investigated.[19] From hybridization studies on 2′-O-propargylated oligonucleotides, they concluded that this modification increases the duplex stability similar to other 2′-modifications.[19]

dx.doi.org/10.1021/jo500392j | J. Org. Chem. 2014, 79, 4423−4437

Table 1. Molecular Masses of Oligonucleotides Measured by MALDI-TOF Mass Spectrometry

Oligonucleotides	M.W. calcd.[a] [u] M.W. found[b] [u]	Oligonucleotides	M.W. calcd.[a] [u] M.W. found[b] [u]
5'-d(TGG GTC AAT ACT) (**27**)	3660.4 3660.1	5'-d(T1G GTC AAT ACT) (**38**)	3713.4 3713.1
5'-d(AGT ATT GAC CCA) (**28**)	3629.4 3629.0	5'-d(AGT ATT G1C CTA) (**39**)	3713.4 3712.9
5'-d(TAG GCC AAT ACT) (**29**)	3629.4 3629.3	5'-d(TAG GTC 1AT ACT) (**40**)	3713.4 3713.0
5'-d(AGT ATT GGC CTA) (**30**)	3660.4 3660.2	5'-d(1GT ATT GAC CTA) (**41**)	3713.4 3714.6
5'-r(UAG GUC AAU ACU) (**31**)	3780.3 3779.3	5'-d(TAG G21C AAT ACT) (**42**)	3698.5 3697.4
5'-r(AGU AUU GAC CUA) (**32**)	3780.3 3779.8	5'-d(AGT ATT GAC C21A) (**43**)	3698.5 3697.4
5'-d(T3G GTC AAT ACT) (**33**)	3698.5 3700.9	5′-d(T11G GTC AAT ACT) (**44**)	3783.6 3783.2
5'-d(AGT ATT G3C CTA) (**34**)	3698.5 3700.0	5'-d(AGT ATT G11C CTA) (**45**)	3783.6 3782.9
5'-d(TAG GTC 3AT ACT) (**35**)	3698.5 3699.2	5'-d(T22G GTC AAT ACT) (**46**)	3729.5 3729.6
5'-d(3GT ATT GAC CTA) (**36**)	3698.5 3698.0	5'-d(T2aG GTC AAT ACT) (**47**)	3659.4 3658.7
5′-d(AGT ATT G2aC CTA) (**37**)	3659.4 3658.7	5'-d(AGT ATT G22C CTA) (**48**)	3729.5 3728.5

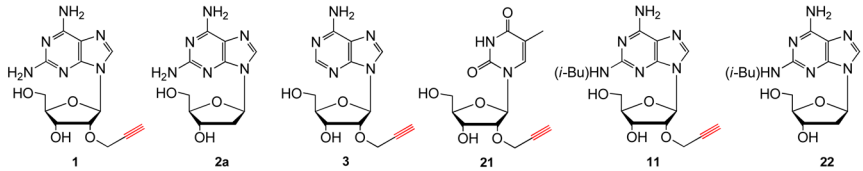

[a]Calculated on the basis of molecular weight as $[M + H]^+$. [b]Determined by MALDI-TOF mass spectrometry as $[M + H]^+$ in the linear positive mode.

We selected 2′-O-propargylated 2-aminoadenosine (**1**) for this study due to the stabilizing properties of 2-aminoadenine replacing adenine in DNA−DNA duplexes or DNA−RNA hybrids. In earlier studies on homopurine−homopyrimidine polyribonucleotide duplexes with 2-aminoadenosine replacing adenosine, a T_m increase of +33 °C was observed.[20] For the corresponding oligodeoxyribonucleotide duplexes, the increment is less but still high (about +12 °C). Later, optical melting experiments on oligodeoxyribonucleotides showed that the situation is more complex with regard to the stabilizing effect of the 2-aminoadenosine−dT base pair in different sequence motifs.[21]

The participation of the 2-amino group of 2-aminoadenosine (**2b**) in a tridentate base pair with dT (bp1) leads to a higher stability than the bidentate dA−dT (bp4), and the stabilizing effect is similar to that of the tridentate dG−dC pair (bp3) (Figure 3). However, due to ups and downs of thermal stability data, this matter is not well understood. Only when we used 2-aminoadenine nucleoside analogues, which have a 7-deazapurine or 8-aza-7-deazapurine skeleton, and a halogen substituent, which were first studied in our laboratory and later used by others, was a pronounced stability increase observed.[11]

In the following, the properties of the propargylated nucleoside **1** along with the related compounds **3**, **11**, **21** and the 2-amino 2′-deoxyribonucleosides **2a** and **22** were investigated with regard to base pair stability (Table 2). Hybridization was studied on DNA−DNA duplexes, as well as on DNA−RNA hybrids having the modification always in the DNA strand, and the

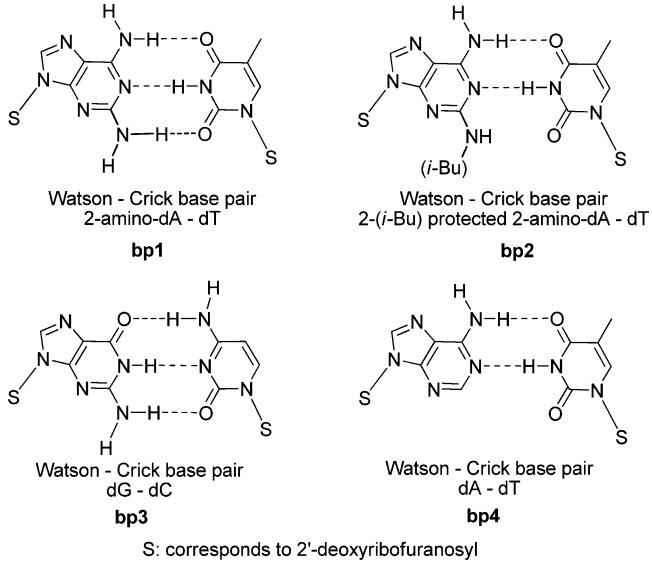

Figure 3. Base pair motifs related to 2-amino-dA−dT, protected 2-amino-dA−dT, dA−dT, and dG−dC.

T_m data are summarized in Table 2. Some propargylated and azido-modified oligonucleotides served later as starting materials for cross-linking reactions using the "stepwise click" reaction (Tables 3 and 4).

dx.doi.org/10.1021/jo500392j | J. Org. Chem. 2014, 79, 4423−4437

Table 2. T_m Values of Modified DNA Duplexes and DNA−RNA Hybrids Containing 2′-*O*-Propargylated Nucleosides[a]

Reference Duplexes							
5′-d(TAG GTC AAT ACT) (**25**) 3′-d(ATC CAG TTA TGA) (**26**)	50.0	5′-d(TAG GTC AAT ACT) (**25**) 3′-r(AUC CAG UUA UGA) (**32**)	46.0	5′-r(UAG GUC AAU ACU) (**31**) 3′-r(AUC CAG UUA UGA) (**32**)	60.0	5′-r(UAG GUC AAU ACU) (**31**) 3′-d(ATC CAG TTA TGA) (**26**)	50.0
DNA Duplexes Upper Strand Modified		**DNA/RNA Hybrids Upper Strand Modified**		**DNA Duplexes Lower Strand Modified**		**DNA/RNA Hybrids Lower Strand Modified**	
5′-d(T2aG GTC AAT ACT) (**47**) 3′-d(ATC CAG TTA TGA) (**26**)	51.5	5′-d(T2aG GTC AAT ACT) (**47**) 3′-r(AUCCAG UUA UGA) (**32**)	47.0	5′-d(TAG GTC AAT ACT) (**25**) 3′-d(ATC C2aG TTA TGA) (**37**)	51.0	5′-r(UAG GUC AAU ACU) (**31**) 3′-d(ATC C2aG TTA TGA) (**37**)	51.0
5′-d(TAG GTC 1AT ACT) (**40**) 3′-d(ATC CAG TTA TGA) (**26**)	50.0	5′-d(TAG GTC 1AT ACT) (**40**) 3′-r(AUCCAG UUA UGA) (**32**)	51.0	5′-d(TAG GTC AAT ACT) (**25**) 3′-d(ATC C1G TTA TGA) (**39**)	48.5	5′-r(UAG GUC AAU ACU) (**31**) 3′-d(ATC C1G TTA TGA) (**39**)	51.5
5′-d(T1G GTC AAT ACT) (**38**) 3′-d(ATC CAG TTA TGA) (**26**)	49.5	5′-d(T1G GTC AAT ACT) (**38**) 3′-r(AUCCAG UUA UGA) (**32**)	49.0	5′-d(TAG GTC AAT ACT) (**25**) 3′-d(ATC CAG TTA TG1) (**41**)	51.0	5′-r(UAG GUC AAU ACU) (**31**) 3′-d(ATC CAG TTA TG1) (**41**)	50.5
5′-d(TAG GTC 3AT ACT) (**35**) 3′-d(ATC CAG TTA TGA) (**26**)	48.0	5′-d(TAG GTC 3AT ACT) (**35**) 3′-r(AUCCAG UUA UGA) (**32**)	47.0	5′-d(TAG GTC AAT ACT) (**25**) 3′-d(ATC C3G TTA TGA) (**34**)	47.0	5′-r(UAG GUC AAU ACU) (**31**) 3′-d(ATC C3G TTA TGA) (**34**)	49.5
5′-d(T11G GTC AAT ACT) (**44**) 3′-d(ATC CAG TTA TGA) (**26**)	49.5	5′-d(T11G GTC AAT ACT) (**44**) 3′-r(AUCCAG UUA UGA) (**32**)	50.0	5′-d(TAG GTC AAT ACT) (**25**) 3′-d(ATC C11G TTA TGA) (**45**)	52.0	5′-r(UAG GUC AAU ACU) (**31**) 3′-d(ATC C11G TTA TGA) (**45**)	52.0
5′-d(T22G GTC AAT ACT) (**46**) 3′-d(ATC CAG TTA TGA) (**26**)	50.5	5′-d(T22G GTC AAT ACT) (**46**) 3′-r(AUCCAG UUA UGA) (**32**)	46.0	5′-d(TAG GTC AAT ACT) (**25**) 3′-d(ATC C22G TTA TGA) (**48**)	53.5	5′-r(UAG GUC AAU ACU) (**31**) 3′-d(ATC C22G TTA TGA) (**48**)	52.0
5′-d(TGG GTC AAT ACT) (**27**) 3′-d(ACC CAG TTA TGA) (**28**)	54.0			5′-d(TAG GCC AAT ACT) (**29**) 3′-d(ATC CGG TTA TGA) (**30**)	55.0		
DNA Duplexes with Modifications within the Base Pair							
5′-d(T1G GTC AAT ACT) (**38**) 3′-d(A21C CAG TTA TGA) (**43**)	49.0	5′-d(TAG G21C AAT ACT) (**42**) 3′-d(ATC C1G TTA TGA) (**39**)	46.0	5′-d(T3G GTC AAT ACT) (**33**) 3′-d(A21C CAG TTA TGA) (**43**)	48.0	5′-d(TAG G21C AAT ACT) (**42**) 3′-d(ATC C3G TTA TGA) (**34**)	44.0
5′-d(T11G GTC AAT ACT) (**44**) 3′-d(A21C CAG TTA TGA) (**43**)	52.0	5′-d(TAG G21C AAT ACT) (**42**) 3′-d(ATC C11G TTA TGA) (**45**)	54.0				

[a]Measured at 260 nm in 1 M NaCl, 100 mM $MgCl_2$, 60 mM Na-cacodylate (pH 7.0) with 2.5 + 2.5 μM single-strand concentration. T_m values were determined from the melting curves by using the software MELTWIN 3.0.

The T_m of the reference RNA−RNA duplex **31**·**32** is 10 °C higher than that of the corresponding DNA−DNA duplex **25**·**26**. The stability of DNA−RNA hybrids (**25**·**32**, **31**·**26**) corresponds to that of the DNA−DNA duplex and not to that of the RNA−RNA duplex. A single modification of oligonucleotide duplexes with 2′-O-propargyl residues has only a minor impact on the thermal stability of DNA−DNA and DNA−RNA duplexes (Table 2). Generally, duplexes incorporating **1** instead of propargylated dA opposite to dT show slightly increased T_m values (+1 °C). Apparently, the 2-amino group of **1** is too basic to act as an efficient proton donor to form a third hydrogen bond with dT. Accordingly, formation of a tridentate base pair of **1** with dT as shown in bp1 is unlikely (Figure 3). This is supported by the finding that duplex **27**·**28** containing a dG−dC base pair (bp3) instead of a dA−dT pair (bp4) shows a significantly higher T_m value compared to duplex **38**·**26** with a **1**−dT base pair. Apparently, bp1 is only formed in a particular environment (e.g., in homopolymers).[22]

Surprisingly, when the 2-amino group was still protected with an isobutyryl residue (**11** or **22**), as in duplexes **44**·**26** and **25**·**45** as well as in **46**·**26** and **25**·**48**, there were few differences in the T_m values compared to the 2-amino unprotected compounds, even under the spatial demand of the isobutyryl residue. Similar observations were already made on other modified oligonucleotides with acetyl groups.[23]

4. Formation of Cross-Linked Duplexes by Stepwise Click Ligation Using the Bifunctional Azide 4. In the next series of experiments, oligonucleotides incorporating 2′-O-propargylated 2-aminoadenosine (**1**) were cross-linked to oligonucleotides containing other propargylated nucleosides to increase duplex stability. Cross-linking was performed between two complementary strands. The cross-links were introduced within base pairs or with proximal propargylated nucleosides of the complementary strand. The click reaction was performed in a stepwise manner with single-stranded azido derivatives prepared by a first-click reaction. This methodology was applied for the following reason: Although it is accepted knowledge that template-assisted reactions occur much faster than those not assisted by the template effect,[24] the situation for terminal and internal cross-linking is different. Cross-linking of terminal azido groups with terminal alkyne residues of preformed DNA duplex is much faster than on individual single strands.[15,24] The situation changes when a cross-link between two complementary strands has to be installed in the center of a duplex and short linkers are employed. This is valid for the formation of cross-links by the bis-click reaction with bifunctional azides in the center of a preformed duplex consisting of long oligonucleotides. In this case, the duplex can have a negative impact on cross-linking. Inspection of the DNA double helix structure clearly indicates that internal cross-links are difficult to form due to steric hindrance. Thus, a positive template effect can be expected only when all components of the bis-click reaction are well-suited in the required space of the DNA duplex. Consequently, when using bis-click conditions (stoichiometric amounts of bis-azide and alkynylated DNA), these effects can cause side reactions. Possibly, the azido-modified DNA strand can react with incompletely functionalized material of the same strand instead of the complementary strand, thus forming homo-DNA duplexes. This unfavorable situation can be circumvented if the stepwise procedure is used either employing chelating bis-azides or using an excess of bis-azide to form a monofunctionalized azido−DNA intermediate.[8,25]

Accordingly, in the first step of the stepwise click reaction, the propargylated oligonucleotides were converted into monofunctionalized azido derivatives using a large excess of azide **4** (ratio ODN/bis-azide 1:15). Usually, 3 to 4 OD of propargylated ODN was dissolved in a mixture of 100 μL of H_2O/MeCN (10:1, v/v), followed by the addition of copper turnings. By this means, the reaction was completed within 3 h.

dx.doi.org/10.1021/jo500392j | J. Org. Chem. 2014, 79, 4423−4437

Table 3. Molecular Masses of Monofunctionalized Oligonucleotides Prepared by the Stepwise Click Reaction

Oligonucleotides	M.W. calcd.[a] [u] M.W. found[b] [u]	Oligonucleotides	M.W. calcd.[a] [u] M.W. found[b] [u]
5'-d(T**19**G GTC AAT ACT) (**49**)	3869.6 3869.6	5'-d(AGT ATT G**19**C CTA) (**54**)	3869.6 3869.0
5'-d(TAG **Gz**TC AAT ACT) (**50**)	3854.6 3857.1	5'-d(AGT ATT GAC C **Tz**A) (**55**)	3854.6 3854.0
5'-d(TAG GTC AA**Tz** ACT) (**51**)	3854.6 3853.7	5'-d(T**Az**G GTC AAT ACT) (**56**)	3854.6 3854.8
5'-d(AGT ATT G**Az**C CTA) (**52**)	3854.6 3853.8	5'-d(AGT ATT **Gz**AC CTA) (**57**)	3854.6 3854.2
5'-d(TAG GTC AAT A**Cz**T) (**53**)	3854.6 3856.0	5'-d(**Az**GT ATT GAC CTA) (**58**)	3854.6 3853.4

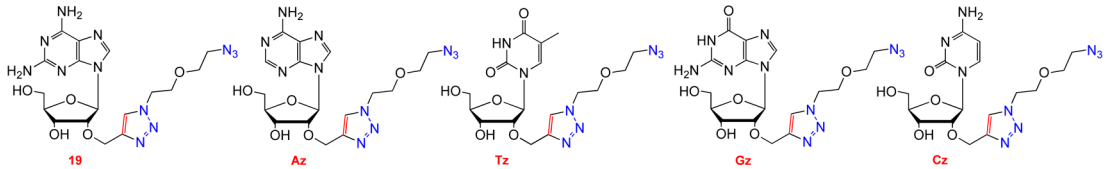

[a]Calculated on the basis of molecular weight as $[M + H]^+$. [b]Determined by MALDI-TOF mass spectrometry as $[M + H]^+$ in the linear positive mode.

Scheme 7. Stepwise Click Reaction of Sugar-Modified DNA[a]

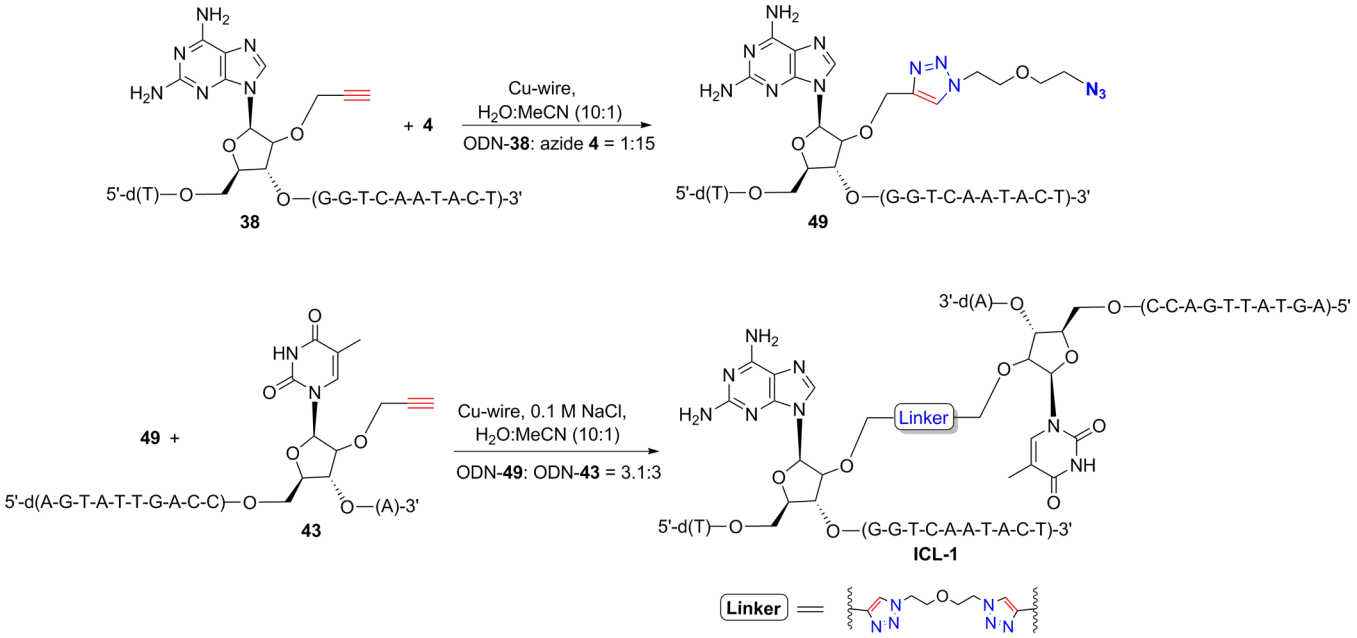

[a]General scheme for the monofunctionalization and cross-linking of oligonucleotides demonstrated for **49** and **ICL-1**.

The sequences of the azido-modified oligonucleotides and their molecular masses are depicted in Table 3.

In the second step, the azido-functionalized ODNs were cross-linked with alkyne-modified complementary duplexes. The alkyne-modified ODN (2−3 OD) was dissolved in 100 μL H_2O/MeCN, then 50 μL of 0.1 M NaCl and monofunctionalized oligonucleotide were added. The monofunctionalized ODN was taken in slight excess to drive the reaction to completion, leading to easy purification. Finally, copper turnings were introduced, and the mixture was stirred in the dark at normal atmosphere for 3 h (Scheme 7). The reaction yield was in the range of 50−60% (for details, see Experimental Section). The structures of monofunctionalized ODNs are given in the Supporting Information (Figure S1). The cross-linked ODNs are listed in Table 4 and were characterized by MALDI-TOF and ion-exchange HPLC (Figure 4; Figure S3, Supporting Information; for detailed structures, see Figure S2, Supporting Information).

It is worth mentioning that the conditions described above using copper turnings and H_2O/MeCN mixtures as reaction medium, a method initially introduced by Jawalekar, is particularly useful as the click reactions (monofunctionalization and cross-linking) were performed quickly and efficiently.[16b] The copper turnings have to be removed after 1 h. Then, the reaction was continued for completion (2 h at rt) without copper turnings. When the copper turnings were kept in the solution for more than 1 h, the final product turned a greenish color, and the yield of the click reactions was greatly reduced.

dx.doi.org/10.1021/jo500392j | J. Org. Chem. 2014, 79, 4423−4437

Table 4. T_m Values of Sugar-Modified Duplexes, Cross-Linked Duplexes, and Hairpins

Modified Duplexes	T_m [°C]	M.W. calcd. M.W. found	Cross-linked Duplexes	T_m [°C]	M.W. calcd.[d] M.W. found[e]
5'-d(T**1**G GTC AAT ACT) (**38**) 3'-d(A**21**C CAG TTA TGA) (**43**)	49.0[a]	--	5'-d(T**1**G GTC AAT ACT) | (**ICL-1**) 3'-d(A**21**C CAG TTA TGA)	79.0[a,c] 71.0[b]	7568.0 7565.9
5'-d(T**3**G GTC AAT ACT) (**33**) 3'-d(A**21**C CAG TTA TGA) (**43**)	47.0[a]	--	5'-d(T**3**G GTC AAT ACT) | (**ICL-2**) 3'-d(A**21**C CAG TTA TGA)	79.0[a,c] 70.5[b]	7553.1 7554.2
5'-d(**21**AG GTC AAT ACT) (**59**) 3'-d(A**21**C CAG TTA TGA) (**43**)	49.0[a]	**59**, 3698.5 **59**, 3697.4	5'-d(**21**AG GTC AAT ACT) ⌞ (**ICL-3**) 3'-d(A**21**C CAG TTA TGA)	79.0[a,c] 72.0[b]	7553.1 7552.1
5'-d(TAG GTC AAT A**23**T) (**60**) 3'-d(ATC CAG TTA TG**3**) (**36**)	48.0[a]	**60**, 3698.5 **60**, 3696.4	5'-d(TAG GTC AAT A**23**T) ⌞ (**ICL-4**) 3'-d(ATC CAG TTA TG**3**)	80.0[a,c] 72.0[b]	7553.1 7550.6
Hairpin			**Hairpin**		
T T TAG GTC AAT ACT T ATC CAG TTA TGA (**H1**) T T	78.0[a,c] 66.0[b]	8871.8 8872.8	pd pd TAG GTC AAT ACT pd ATC CAG TTA TGA (**H2**) pd pd	77.0[a] 63.0[b]	8041.0 8041.9
Modified Duplexes			**Cross-linked Duplexes**		
5'-d(TAG G**21**C AAT ACT) (**42**) 3'-d(ATC C**3**G TTA TGA) (**34**)	44.0[a]	--	5'-d(TAG G**21**C AAT ACT) | (**ICL-5**) 3'-d(ATC C**3**G TTA TGA)	72.5[a] 70.0[b]	7553.1 7552.2
5'-d(TAG G**21**C AAT ACT) (**42**) 3'-d(ATC C**1**G TTA TGA) (**39**)	46.0[a]	--	5'-d(TAG G**21**C AAT ACT) | (**ICL-6**) 3'-d(ATC C**1**G TTA TGA)	73.0[a] 70.0[b]	7568.0 7567.5
5'-d(TAG **24**TC AAT ACT) (**61**) 3'-d(ATC **23**AG TTA TGA) (**62**)	48.0[a]	**61**, 3698.5 **61**, 3696.9 **62**, 3698.5 **62**, 3697.1	5'-d(TAG **24**TC AAT ACT) | (**ICL-7**) 3'-d(ATC **23**AG TTA TGA)	74.0[a]	7553.1 7552.4
5'-d(TAG GTC AA**21** ACT) (**63**) 3'-d(ATC CAG TTA TG**3**) (**36**)	46.0[a]	**63**, 3698.5 **63**, 3697.4	5'-d(TAG GTC AA**21** ACT) ⌞ (**ICL-8**) 3'-d(ATC CAG TTA TG**3**)	74.0[a]	7553.1 7552.9
5'-d(TAG GTC **3**AT ACT) (**35**) 3'-d(ATC C**3**G TTA TGA) (**34**)	44.0[a]	--	5'-d(TAG GTC **3**AT ACT) ⌞ (**ICL-9**) 3'-d(ATC C**3**G TTA TGA)	69.0[a] 66.0[c]	7553.1 7551.7
5'-d(TAG **24**TC AAT ACT) (**61**) 3'-d(ATC C**3**G TTA TGA) (**34**)	45.0[a]	--	5'-d(TAG **24**TC AAT ACT) ⌞ (**ICL-10**) 3'-d(ATC C**3**G TTA TGA)	69.0[a]	7553.1 7551.6
5'-d(TAG GT**23** AAT ACT) (**64**) 3'-d(ATC CA**24** TTA TGA) (**65**)	45.0[a]	**64**, 3698.5 **64**, 3696.3 **65**, 3698.5 **65**, 3697.2	5'-d(TAG GT**23** AAT ACT) | (**ICL-11**) 3'-d(ATC CA**24** TTA TGA)	68.5[a] 64.0[b]	7553.1 7552.2
5'-d(T**3**G GTC AAT ACT) (**33**) 3'-d(ATC C**3**G TTA TGA) (**34**)	45.0[a]	--	5'-d(T**3**G GTC AAT ACT) ⌞ (**ICL-12**) 3'-d(ATC C**3**G TTA TGA)	67.0[a] 61.0[b]	7553.1 7552.0

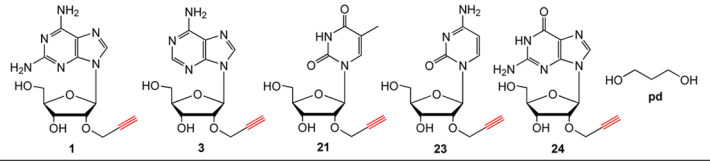

[a]Measured at 260 nm in 1 M NaCl, 10 mM $MgCl_2$, 10 mM Na-cacodylate (pH 7.0) with 2.5 + 2.5 μM single-strand concentration for non-cross-linked oligonucleotides and 5 μM for cross-linked oligonucleotides. For hairpins, 5 μM of oligonucleotide was used. [b]In 50 mM NaCl, 10 mM Na_3PO_4, 0.1 mM EDTA with 2.5 + 2.5 μM single-strand concentration for non-cross-linked oligonucleotides and 5 μM for cross-linked oligonucleotides. For hairpins, 5 μM of oligonucleotide was used. [c]Data taken from visual inspection of the melting curve. [d]Calculated on the basis of molecular weight as $[M + H]^+$. [e]Determined by MALDI-TOF mass spectrometry as $[M + H]^+$ in the linear positive mode. **pd** corresponds to 1,3-propanediol. All cross-linked oligonucleotides are shown in the Supporting Information (Figure S2). T_m values were determined from the melting curves by using the software MELTWIN version 3.0.

Figure 4a–c displays ion-exchange HPLC profiles demonstrating the various mobilities of the alkynylated, azido-modified, and cross-linked oligonucleotides, which were purified by reversed-phase HPLC (for details, see Experimental Section). Figure 4d shows the ion-exchange profile of an artificial mixture of all components. Azido-modified oligonucleotides with identical base

dx.doi.org/10.1021/jo500392j | J. Org. Chem. 2014, 79, 4423–4437

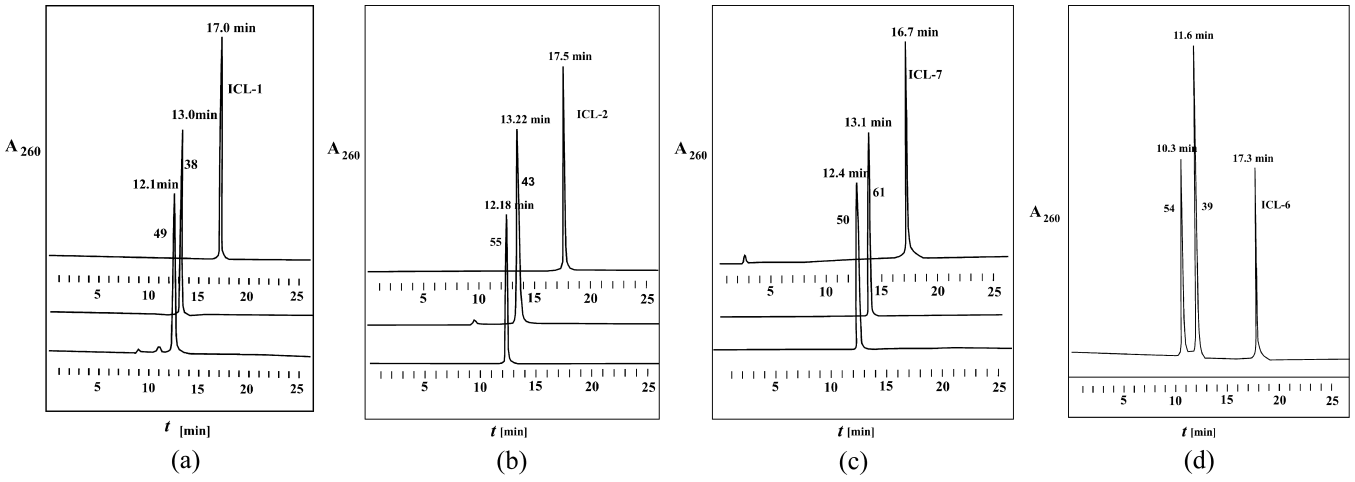

Figure 4. Ion-exchange HPLC elution profiles of (a) monofunctionalized ODN-**49**, ODN-**38**, and interstrand cross-linked ODN **ICL-1**; (b) monofunctionalized ODN-**55**, ODN-**43**, and interstrand cross-linked ODN **ICL-2**; (c) monofunctionalized ODN-**50**, ODN-**61**, and interstrand cross-linked ODN **ICL-7**; (d) artificial mixture of monofunctionalized ODN-**54**, ODN-**39**, and interstrand cross-linked ODN **ICL-6**. Ion-exchange chromatography was performed on a 4 × 250 mm DNA Pac PA-100 column, using the following buffer system: (A) 25 mM Tris-HCl, 10% MeCN, pH 7.0; (B) 25 mM Tris-HCl, 1.0 M NaCl, and 10% MeCN, pH 7.0. Elution gradient: 0−30 min 20−80% B in A with a flow rate of 0.75 mL min^{-1}.

composition can be cleanly separated from the alkynylated precursor molecules. Cross-linked duplexes migrate significantly slower. The reaction shown in Scheme 7 is not limited to propargylated 2-aminoadenosine. The stepwise click reaction was also performed on propargylated derivatives of the canonical nucleosides. A complete set of ion-exchange profiles of propargylated, monofunctionalized, and cross-linked ODNs is given in the Supporting Information (Figure S3; for reaction profiles, see Figures S4 and S5).

5. Thermal Stability of Cross-Linked Duplexes with Cross-Links between 2′-O-Propargylated 2-Aminoadenosine and Other Modified Nucleoside Residues. Different methods have been employed for cross-linking DNA.[26] Our laboratory has reported on site-specific cross-linking of oligonucleotides in which terminal triple bonds on the side chain of a nucleobase were clicked together and the length of the linker, the ligation position, or both were altered. In some cases, T_m values of cross-linked duplexes were about 25 °C higher than those for the non-cross-linked hybrids; in other cases, the effect was lower.[15] Later, cross-linking oligonucleotides with 2′-O-propargylated sugar residues in DNA with parallel and antiparallel chain orientation were reported.[9] In this work, 2′-O-propargylated nucleosides were introduced in both strands of oligonucleotide duplexes (Table 4, left column). Cross-linked duplexes show significantly increased T_m values (Table 4, right column). This is valid not only for cross-links with 2-aminoadenosine but also for other nucleoside combinations.

From Table 4 (upper part), it is apparent that T_m values of cross-linked duplexes ligated at the terminus of the duplex (**ICLs 1−4**) are around 80 °C. Moving the ligation site toward the center of the duplex leads to decreased duplex stability (**ICLs 5−12**; Table 4, lower part). Thus, the connectivity of cross-linked residues plays a key role in duplex stability.

From the physical point of view, the thermal stability of a cross-linked duplex increases simply by the change of the molecularity during melting or formation. The non-cross-linked duplex dissociates in a bimolecular reaction to yield single-stranded species, while in the cross-linked duplexes, base pair melting occurs without strand separation.

The melting of a cross-linked duplex with a terminal ligation site can be described as the melting of a hairpin. We synthesized two hairpins (**H1** and **H2**) to analyze this matter. The hairpins consist of the sequence motif of the duplex **25** and **26** (Table 1) in the stem region and a loop of either five dT (**H1**) or five propanediol (**H2**) residues. These two hairpins exhibit similar T_m values (77 and 78 °C). All four oligonucleotides with cross-links at the terminus (**ICLs 1−4**) show slightly higher T_m values than the two hairpins **H1** and **H2**, in particular at low salt conditions. This reveals that not only the change of the molecularity during the melting process of cross-linked duplexes vs non-cross-linked duplexes but also structural changes induced by the cross-link can have an effect on the stability of the molecule. In the case of cross-linked duplexes with terminal ligation sites, this effect is positive; for cross-linked duplexes with internal ligation sites, a decreased thermal stability is often observed. For cross-linked duplexes with lower stability, see Table 4 (right column, lower part), and for those with higher thermal stability, see Table 4 (right column, upper part).

To support these findings, molecular dynamic simulation studies (AMBER force field, HyperChem 8.0; Hypercube, Inc., Gainesville, FL, 2001) were conducted on **ICL-1** and **ICL-6** and are displayed in Figure 5. From the figure, it is evident that a long run of base pairs is still intact in **ICL-1** (terminal cross-link). For **ICL-6** (internal cross-link), two shorter regions of matched base pairs exist. A closer inspection shows that in **ICL-1** as well as in **ICL-6** the base pair of the cross-link and at least one next to it are opened. Nevertheless, the disturbed base pair is always replaced by a covalent linkage of the strands. A higher stability is observed for duplexes with terminal cross-links compared to those with central ligation sites, which might result from a stronger distortion of the helix for central cross-links, changes in stacking interactions, or a combination thereof. Furthermore, helix hydration and ion-binding might be affected in a different manner. In turn, this effect depends on the participating nucleosides, their distance in the duplex, and cross-linking within a base pair or between nucleosides residues in proximal or more distant positions. Also, the length of the linker is of utmost importance. Unpredictable T_m changes might occur

dx.doi.org/10.1021/jo500392j | J. Org. Chem. 2014, 79, 4423−4437

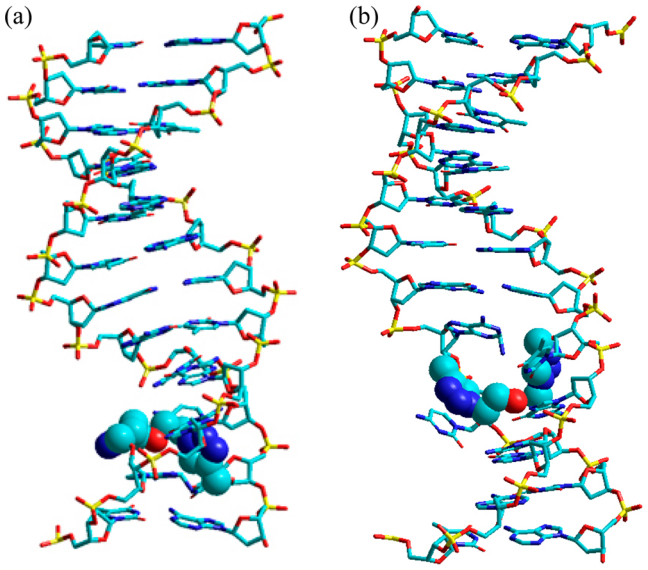

Figure 5. Molecular models of (a) **ICL-1** with a terminal cross-link; (b) **ICL-6** with a cross-link at the center of the duplex. The modification sites are presented as colored, space-filling, overlapping spheres. The models were constructed using HyperChem 8.0 and energy minimized by using AMBER calculations.

when the cross-linked duplex has the choice to form another set of base pairs.

We recognized that the salt dependence of the T_m values is rather different between duplexes, hairpins, and cross-linked species. Figure 6 compares melting profiles of the parent duplex **25·26**, the corresponding hairpin **H1**, and the cross-linked duplex with terminal (**ICL-1**) or central (**ICL-6**) ligation sites at high salt and low salt measuring conditions (for additional melting curves measured under high and low salt conditions, see Supporting Information, Figures S5 and S6).

From Figure 6, it is obvious that the duplex **25·26** and the hairpin **H1**, as well as the cross-linked duplex with the near terminal ligation site (**ICL-1**) connecting propargylated 2-aminoadenosine with propargylated dT, show similar steep melting curves with high cooperativity. In contrast, the duplex with the cross-link near the center (**ICL-6**) shows a less cooperative melting, which is particularly visible under high salt conditions. Furthermore, the duplex with the central ligation site began melting with a continuous increase of the UV-absorbance followed by cooperative melting. The hypochromicity of cooperative melting was reduced over that observed for the corresponding duplexes or hairpins under the same high salt conditions. The cross-linked duplex with a terminal ligation site (**ICL-1**) shows a steep melting profile similar to that of hairpin **H1** but has a different salt dependence.

CONCLUSION AND OUTLOOK

A protecting group strategy for 2′-O-propargylated 2-amino-adenosine (**1**) containing two amino groups of rather different reactivities was developed successfully, and various new phosphoramidites were prepared as building blocks for solid phase oligonucleotide synthesis. Hybridization experiments with a series of oligonucleotide duplexes containing 2,6-diaminopurine as nucleobase showed no significant duplex stabilization over those containing adenine. Consequently, the formation of a tridentate base pair was ruled out. An isobutyryl group protecting

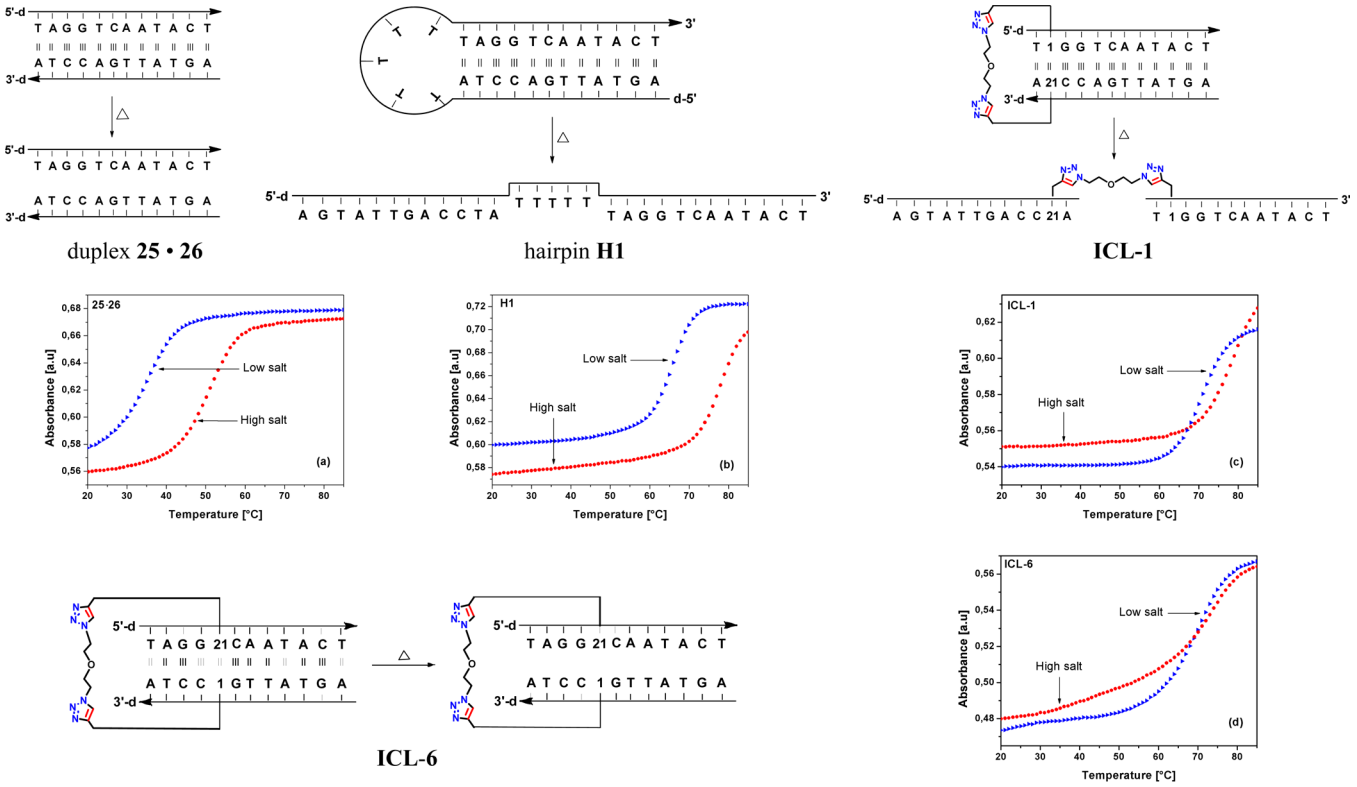

Figure 6. Melting profiles of the duplex **25·26**, the hairpin **H1**, and the cross-linked duplexes **ICL-1** and **ICL-6**. T_m curves in red represent heating profiles measured in 1 M NaCl, 100 mM $MgCl_2$, 60 mM sodium-cacodylate. T_m curves in blue represent heating profiles measured in 50 mM NaCl, 10 mM sodium-phosphate, 0.1 mM EDTA buffer. Δ corresponds to thermal melting.

dx.doi.org/10.1021/jo500392j | J. Org. Chem. 2014, 79, 4423−4437

Table 5. ^{13}C NMR Chemical Shifts of 2-Aminoadenosine Derivatives[a,b]

	C(2)[c]	C(4)	C(5)	C(6)[c]	C(8)	C≡C	CH_2	C(1′)	C(2′)	C(3′)	C(4′)	C(5′)	C=O	$CHMe_2$	CH
1[e]	156.2	151.4	113.4	160.1	135.8	79.7	56.9	86.2	79.8	68.9	84.8	61.6			
						77.6									
2a[f]	156.1	151.2	113.5	160.0	135.7			83.1	39.4	71.0	87.6	61.9			
7	160.0	153.3	119.3	160.1	137.3	77.7	56.8	84.5	79.8	68.9	86.1	61.4			
						79.8									
8	152.2	152.6	121.0	149.9	141.7			83.1[c]	*d*	70.7	87.9	61.7	175.6		34.2
													175.2		34.3
9	152.2	152.4	121.0	149.9	141.7			83.2[c]	*d*	70.5	86.2	64.3	175.5		29.6
													175.0		34.2
11	152.9	150.3	116.1	156.1	138.5	79.9	57.0	84.8	80.1	68.8	86.1	61.3	175.0	19.4	34.1
						77.6								19.3	
12	152.2	152.7	122.1	159.8	140.1	79.8	57.1	84.8	80.2	68.7	86.1	61.2	174.9	19.3	34.3
						77.5								19.2	
13	152.8	152.1	122.2	159.8	139.9	79.9	57.3	85.4	79.8	69.1	83.8	63.9	174.8	19.3	34.2
						77.6								19.2	
15	152.1	149.9	115.9	155.9	138.4	79.6	56.8	85.8	79.8	68.5	84.8	61.0	168.3		
						77.3	58.3								
16	151.8	149.9	120.3	152.6	141.6	80.2	58.5	85.2	79.8	68.7	86.1	61.1	175.5	19.2	34.3
						77.6	57.2						169.2		
17	151.6	149.7	119.9	152.2	141.3	79.7	58.2	85.6	79.5	68.9	85.3	63.6	175.2	19.0	34.1
						77.4	57.2						168.8		
19	156.2	151.4	113.4	160.1	135.9		49.8	85.1	80.2	69.0	86.0	61.6			
							49.2								
20	156.2	151.4	113.4	160.1	135.9		48.6	85.1	80.1	69.0	86.1	61.6			
							49.0								

[a]Measured in DMSO-d_6 at 298 K. [b]Purine numbering. [c]Tentative. [d]Superimposed by DMSO. [e]Reference no. 9. [f]Reference no. 27.

the 2-amino function does not destabilize DNA−DNA and DNA−RNA duplexes, showing that this group is well accommodated in complementary duplexes. Cross-linking oligonucleotides containing 2′-O-propargylated 2-aminoadenosine (**1**) led to significant duplex stabilization (T_m = 79 °C for **ICL-1** and 73 °C for **ICL-6** compared to the reference duplex **25·26**, T_m = 50 °C). These cross-linked duplexes were prepared in a stepwise manner using copper turnings as a catalyst. It was shown that duplex stabilization by cross-links does not result simply from a molecularity change from duplex to hairpin melting but also was influenced by the ligation position. Terminal ligation led to higher melting duplexes than hairpins, while duplexes with central ligation sites were less stable than hairpins due to helix distortion. With the help of the stepwise click procedure, any DNA strand with an alkynyl side chain (independent of the position) can be converted into an azido DNA. This applies to the formation of homodimers and heterodimers. Azido DNA can be connected to any other alkynylated biomolecule and can be used for the construction of supramolecular assemblies and nanoscopic devices.

EXPERIMENTAL SECTION

General Methods and Materials. All chemicals and solvents were of laboratory grade as obtained from commercial suppliers and were used without further purification. Thin-layer chromatography (TLC) was performed on TLC aluminum sheets covered with silica gel 60 F254 (0.2 mm). Flash column chromatography (FC): silica gel 60 (40−60 μM) at 0.4 bar. UV spectra were recorded on a spectrophotometer: λ_{max} in nm, ε in dm^3 mol^{-1} cm^{-1}. NMR spectra were measured at 300.15 MHz for ^{1}H, 75.48 MHz for ^{13}C, and 121.52 MHz for ^{31}P. The *J* values are given in hertz (Hz); δ values in parts per million (ppm) relative to Me_4Si as an internal standard. For NMR spectra recorded in DMSO-d_6, the chemical shift of the solvent peak was set to 2.50 ppm for ^{1}H NMR and 39.50 ppm for ^{13}C NMR. The ^{13}C NMR signals were assigned on the basis of DEPT-135 and ^{1}H−^{13}C gated-decoupled NMR spectra (Table 5; for coupling constants, see Table S1, Supporting Information). Reversed-phase HPLC was carried out on a 250 × 4 mm RP-18 LiChrospher 100 column with an HPLC pump connected with a variable wavelength monitor, a controller, and an integrator. Gradients used for HPLC chromatography: A = MeCN; B = 0.1 M (Et_3NH)OAc (pH 7.0)/MeCN, 95:5. Conditions: (I) 3 min 15% A in B, 12 min 15−50% A in B, and 5 min 50−10% A in B, flow rate 0.7 mL min^{-1}; (II) 0−25 min 0−20% A in B, flow rate 0.7 mL min^{-1}. Melting curves were measured with a UV−vis spectrophotometer equipped with a thermoelectrical controller with a heating rate of 1 °C/min. The T_m values were determined from the melting curves using the software MELTWIN, version 3.0 (J. A. McDowell, 1996). ESI-TOF mass spectra of the nucleosides were measured with a Micro-TOF spectrometer. Molecular masses of oligonucleotides were determined by MALDI-TOF mass spectrometry in the linear positive mode with 3-hydroxypicolinic acid (3-HPA) as a matrix (Tables 1, 3, and 4).

Synthesis, Purification, and Characterization of Oligonucleotides. The syntheses of oligonucleotides **25**−**48** and **59**−**65** were performed on a DNA synthesizer at a 1 μmol scale (trityl-on mode) using the phosphoramidites **10**, **14**, and **18** and the phosphoramidites of 2′-*O*-propargyladenosine, 2′-*O*-propargylguanosine, 2′-*O*-propargylthymidine, 2′-*O*-propargylcytidine, and 1,3-propanediol, as well as the standard phosphoramidite building blocks following the synthesis protocol for 3′-*O*-(2-cyanoethyl)phosphoramidites (user's manual for the 392 and 394 DNA synthesizer, Applied Biosystems, Weiterstadt, Germany). After cleavage from the solid support, the oligonucleotides were deprotected in 25% aqueous ammonia solution for 18 h at 60 °C. The isobutyryl residue of the 2-amino group of 2-amino-2′-deoxyadenosine (**2a**) and the 2′-O-propargylated derivative **1** (phosphoramidites **10** and **14**) withstands the standard deprotection conditions. Therefore, this group was cleaved under harsh conditions using $MeNH_2$/aq. NH_3 (1:1, v/v, at 60 °C for 1 h). Then, the oligonucleotides were dried and purified. The purification of the "trityl-on" oligonucleotides was carried out on reversed-phase HPLC

dx.doi.org/10.1021/jo500392j | J. Org. Chem. 2014, 79, 4423−4437

(RP-18 column; gradient system I). The purified "trityl-on" oligonucleotides were treated with 2.5% of $Cl_2CHCOOH/CH_2Cl_2$ for 5 min at 0 °C to remove the dimethoxytrityl residues. The detritylated oligomers were purified by reversed-phase HPLC (gradient II). The oligomers were desalted on a short column using distilled water for elution of salt, while the oligonucleotides were eluted with H_2O/MeOH (2:3). The solvent was evaporated using a Speed Vac evaporator to yield colorless solids, which were then frozen at −24 °C. The molecular masses of the oligonucleotides were determined by MALDI-TOF mass spectrometry in the linear positive mode. Extinction coefficients ε_{260} (H_2O) of nucleosides are dA, 15 400; dG, 11 700; dT, 8800; dC, 7300; **3**, 14 800 (MeOH); **21**, 8600 (MeOH); **23**, 8200 (MeOH); **24**, 13 000 (MeOH). For the extinction coefficients of 2-aminoadenosine derivatives, see Supporting Information (Table S2).

N^6-[(Di-*n*-butylamino)methylidene]-9-[2-*O*-(propargyl)-β-D-ribofuranosyl]purin-2,6-diamine (7). Compound **1** (0.25 g, 0.78 mmol) was dissolved in MeOH; then *N*,*N*-dibutylaminomethylidene dimethylacetal (500 μL, 2.14 mmol) was added and the solution was stirred at 40 °C for 1 h. The solvent was removed, and the remaining residue was adsorbed on silica gel and subjected to FC (silica gel, CH_2Cl_2/MeOH, 9:1), affording compound **7** (0.147 g, 41%) as a colorless solid. TLC (silica gel, CH_2Cl_2/MeOH, 90:10) R_f 0.4. λ_{max} (MeOH)/nm 253 (ε/dm^3 mol^{-1} cm^{-1} 13 900), 279 (14 500), 325 (20 600). ^{1}H NMR (DMSO-d_6, 300 MHz): δ 0.87−0.94 (m, 6H, 2 × CH_3), 1.26−1.36 (m, 4H, CH_2), 1.54−1.61 (m, 4H, 2 × CH_2), 3.34 (m, superimposed by DMSO, NCH_2), 3.38 (t, *J* = 2.1 Hz, 1H, C≡CH), 3.53−3.63 (m, 4H, 2 x C5′−H, NCH_2), 3.92−3.95 (m, 1H, C4′−H), 4.15−4.32 (m, 3H, OCH_2, C3′−H), 4.53 (dd, *J* = 4.8 Hz, *J* = 5.1 Hz, 1H, C2′−H), 5.30 (m, 2H, C5′−OH, C3′−OH), 5.90 (d, *J* = 6.3 Hz, 1H, C1′−H), 6.00 (br s, 2H, 2-NH_2), 8.04 (s, 1H, C8−H), 8.79 (s, 1H, N=CH). ESI-TOF *m*/*z* calcd for $C_{22}H_{33}N_7O_4$ $[M + H]^+$, 460.2667; found, 460.2657.

9-(2-Deoxy-β-D-*erythro*-pentofuranosyl)-N^2,N^6-diisobutyryl-purin-2,6-diamine (8). Compound **2a** (0.5 g, 1.88 mmol) was dried by repeated coevaporation with pyridine (3 × 5 mL) and dissolved in pyridine (20 mL). Then, trimethylsilyl chloride (1.9 g, 2.26 mL, 17.42 mmol) was added, and the solution was stirred at rt for 15 min. Then, isobutyryic chloride (1.62 g, 1.60 mL, 15.2 mmol) was added dropwise over a period of 5 min, and the reaction mixture was stirred at rt for 3 h. After completion of the reaction (TLC monitoring), the reaction mixture was cooled in an ice-bath, H_2O (5 mL) was added, and, subsequently, 5 min later, 28% aq ammonia (5 mL) was introduced. Stirring was continued for 30 min at rt. The solvent from the reaction mixture was evaporated, and the remaining oily residue was coevaporated with toluene (3 × 10 mL) and subjected to FC (silica gel, CH_2Cl_2/MeOH, 90:10) to give compound **8** (0.474 g, 62%) as a colorless solid. TLC (silica gel, CH_2Cl_2/MeOH, 90:10) R_f 0.6. λ_{max} (MeOH)/nm 265 (ε/dm^3 mol^{-1} cm^{-1} 11 500), 287 (11 200). ^{1}H NMR (DMSO-d_6, 300 MHz): δ 1.07−1.13 (m, 6H, 2 x CH_3), 2.26−2.34 (m, 1H, C2′−H), 2.69−2.78 (m, 1H, C2′−H), 2.85−2.92 (m, 1H, CH), 2.99−3.08 (m, 1H, CH), 3.49−3.64 (m, 2H, 2 x C5′−H), 3.84−3.88 (m, 1H, C4′−H), 4.43−4.44 (m, 1H, C3′−H), 4.91 (t, *J* = 5.4 Hz, 1H, C5′−OH), 5.33 (d, *J* = 4.2 Hz, 1H, C3′−OH), 6.36 ('t', *J* = 6.6 Hz, 1H, C1′−H), 8.51 (s, 1H, C8−H), 10.35 (br s, 1H, NH), 10.51 (br s, 1H, NH). ESI-TOF *m*/*z* calcd for $C_{18}H_{26}N_6O_5$ $[M + Na]^+$, 429.1857; found, 429.1857.

9-[2-Deoxy-5-*O*-(4,4′-dimethoxytrityl)-β-D-*erythro*-pentofuranosyl]-N^2,N^6-diisobutyryl-purin-2,6-diamine (9). Compound **8** (0.30 g, 0.74 mmol) was dried by repeated coevaporation with dry pyridine (3 × 10 mL). The residue was dissolved in dry pyridine (5 mL), and the mixture was stirred with 4,4′-dimethoxytrityl chloride (0.400 g, 1.18 mmol) until the starting material was completely consumed (TLC monitoring). Then, the reaction mixture was diluted with CH_2Cl_2 (20 mL) and washed with 5% aq $NaHCO_3$ solution (20 mL) and water (20 mL). The organic layer was dried over Na_2SO_4, the solvent was evaporated under reduced pressure, and the residue was subjected to FC (silica gel, CH_2Cl_2/acetone, 1:1). Evaporation of the main zone afforded **9** (0.30 g, 58%) as a pale yellow foam. TLC (silica gel, CH_2Cl_2/acetone, 1:1) R_f 0.4. λ_{max} (MeOH)/nm 268sh (ε/dm^3 mol^{-1} cm^{-1} 16 200), 276 (16 700). ^{1}H NMR (DMSO-d_6, 300 MHz): δ 1.05−1.14 (m, 6H, CH_3), 2.32−2.41 (m, 1H, C2′−H), 2.83−2.92 (m, 2H, C2′−H, CH), 3.00−3.15 (m, 2H, C5′−H, CH), 3.26−3.32 (m, 1H, C5′−H), 3.69, 3.71 (2s, 6H, 2 × OCH_3), 3.94−3.97 (m, 1H, C4′−H), 4.52−4.55 (m, 1H, C3′−H), 5.34 (d, *J* = 4.5 Hz, 1H, C3′−OH), 6.39 ('t', *J* = 6.3 Hz, 1H, C1′−H), 6.37−6.41 (m, 1H, 4H, Ar−H), 7.16−7.19 (m, 7H, Ar−H), 7.29−7.32 (m, 2H, Ar−H) 8.40 (s, 1H, C8−H), 10.30 (br s, 1H, NH), 10.52 (br s, 1H, NH). ESI-TOF *m*/*z* calcd for $C_{39}H_{44}N_6O_7$ $[M + Na]^+$, 731.3164; found, 731.3164.

9-[2-Deoxy-5-*O*-(4,4′-dimethoxytrityl)-β-D-*erythro*-pentofuranosyl]-N^2,N^6-diisobutyryl-purin-2,6-diamine 3′-(2-Cyanoethyl)-*N*,*N*-diisopropylphosphoramidite (10). To a solution of compound **9** (0.30 g, 0.42 mmol) in dry CH_2Cl_2 (10 mL) were added (*i*-Pr)$_2$NEt (0.097 g, 125 μL, 0.72 mmol) and 2-cyanoethyl diisopropylphosphoramidochloridite (0.13 g, 125 μL, 0.56 mmol), and the reaction mixture was stirred for 15 min at rt. Then, the reaction mixture was diluted with CH_2Cl_2 (30 mL), poured into 5% $NaHCO_3$ solution (20 mL), and extracted with CH_2Cl_2 (3 × 20 mL). The combined organic layers were dried over Na_2SO_4, and the solvent was evaporated. The residual foam was applied to FC (silica gel, CH_2Cl_2/acetone, 80:20). Evaporation of the main zone afforded **10** (0.277 g, 73%) as a colorless foam. TLC (silica gel, CH_2Cl_2/acetone, 80:20) R_f 0.5, 0.6. ^{31}P NMR ($CDCl_3$, 121.5 MHz): 148.77. ESI-TOF *m*/*z* calcd for $C_{48}H_{62}N_8O_8P$ $[M + H]^+$, 909.4423; found, 909.4423.

9-[(2-*O*-propargyl)-β-D-ribofuranosyl]purin-2,6-diamine (1) and 9-[(3-*O*-propargyl)-β-D-ribofuranosyl]purin-2,6-diamine (6) from 3′,5′-(1,1,3,3-Tetraisopropyl-1,3-disiloxan-1,3-yl)-9-(β-D-ribofuranosyl)purin-2,6-diamine (5). Compound **5**[13a] (0.5 g, 0.95 mmol) was dissolved in anhydrous DMF (10 mL) under argon atmosphere. The solution was cooled to 5 °C, and NaH (0.038 g, 1.28 mmol, 60% dispersion in mineral oil) was added, followed by the addition of TBAI (0.16 g, 0.42 mmol) and propargyl bromide (0.14 g, 105 μL, 1.18 mmol). The reaction mixture was allowed to stir for 20 min at 55 °C. After completion of the reaction (TLC monitoring), the solvent was evaporated under reduced pressure. The residual suspension was dissolved in THF (10 mL) and treated with 0.1 M TBAF in THF (8 mL). The resulting mixture was stirred at rt for 1 h. The solvent was evaporated under reduced pressure, and the remaining residue was subjected to FC (CH_2Cl_2/MeOH, 95:5). From the faster migrating zone, 9-[(2-*O*-propargyl)-β-D-ribofuranosyl]-purin-2,6-diamine (**1**) was obtained as a colorless foam (0.2 g, 66%). TLC (silica gel, CH_2Cl_2/MeOH, 90:10) R_f 0.6. λ_{max} (MeOH)/nm 256 (ε/dm^3 mol^{-1} cm^{-1} 9 400), 260 (8 800), 281 (10 900). Anal. Calcd for $C_{13}H_{16}N_6O_4$ (320.3): C, 48.75; H, 5.03; N, 26.24. Found: C, 48.62; H, 5.10; N, 26.09. From the slower migrating zone, 9-[(3-*O*-propargyl)-β-D-ribofuranosyl]purin-2,6-diamine (**6**) was isolated as colorless solid (0.023 g, 8%). TLC (silica gel, CH_2Cl_2/MeOH, 90:10) R_f 0.5. λ_{max} (MeOH)/nm 260 (ε/dm^3 mol^{-1} cm^{-1} 9 800), 281 (11 400). Anal. Calcd for $C_{13}H_{16}N_6O_4$ (320.3): C, 48.75; H, 5.03; N, 26.24. Found: C, 48.93; H, 5.15; N, 26.10. The analytical data of compounds **1** and **6** are identical to reported values.[9]

N^2-Isobutyryl-9-[2-*O*-(propargyl)-β-D-ribofuranosyl]purin-2,6-diamine (11). Compound **1** (0.2 g, 0.62 mmol) was dried by repeated coevaporation with pyridine, (3 × 5 mL) and dissolved in pyridine (8 mL). Trimethylsilyl chloride (0.34 g, 0.4 mL, 3.12 mmol) was added and the mixture was stirred at rt for 15 min. Then, the solution was cooled to −20 °C, isobutyryl chloride (0.073 g, 0.072 mL, 0.68 mmol) was added dropwise over 5 min, and the reaction mixture was stirred at −20 °C for 2.5 h followed by 1 h at rt. After completion of the reaction (TLC monitoring), the reaction mixture was cooled in an ice-bath, ethanol (2 mL) was added, and subsequently, 5 min later, 28% aq ammonia was added. Stirring was continued for 30 min at rt. The solvent from the reaction mixture was evaporated, and the resulting oily residue was coevaporated with toluene and subjected to FC (silica gel, CH_2Cl_2/MeOH, 95:5) to give compound **11** (0.158 g, 65%) as a colorless solid. TLC (silica gel, CH_2Cl_2/MeOH, 90:10) R_f 0.4. λ_{max} (MeOH)/nm 271 (ε/dm^3 mol^{-1} cm^{-1} 15 800). ^{1}H NMR (DMSO-d_6, 300 MHz): δ 1.04−1.07 (2 s, 6H, 2 × CH_3), 2.79−2.88 (m, 1H, CH), 3.37 (t, *J* = 2.1 Hz, 1H, C≡CH), 3.53−3.58 (m, 1H, C5′−H), 3.61−3.66 (m, 1H, C5′−H), 3.92−3.96 (m, 1H, C4′−H),

dx.doi.org/10.1021/jo500392j | J. Org. Chem. 2014, 79, 4423−4437

4.24 (d, J = 2.4 Hz, 1H, OCH_2), 4.27 (d, J = 2.4 Hz, 1H, OCH_2), 4.32−4.37 (m, 1H, C3′−H), 4.56 (t, J = 5.4 Hz, 1H, C2′−H), 5.10 (t, J = 5.4 Hz, 1H, C5′−OH), 5.31 (d, J = 5.1 Hz, 1H, C3′−OH), 5.95 (d, J = 6.3 Hz, 1H, C1′−H), 7.24 (br s, 2H, 6-NH_2), 8.26 (s, 1H, C8−H), 9.85 (s, 1H, NH). ESI-TOF m/z calcd for $C_{17}H_{22}N_6O_5$ $[M + Na]^+$, 413.1544; found, 413.1539.

N^6-Dibutylaminomethylidene-N^2-isobutyryl-9-[2-*O*-(propargyl)-β-D-ribofuranosyl]purine (12). Compound **11** (0.35 g, 0.90 mmol) was dissolved in methanol (10 mL) and treated with *N*,*N*-dibutylformamid dimethylacetal (1.5 mL) under argon atmosphere at rt for 2 h. The solution was evaporated, and the remaining oily residue was applied to FC (petroleum ether/EtOAc, 4:1, 500 mL; then CH_2Cl_2/MeOH, 95:5) to give compound **12** (0.38 g, 80%) as a colorless foam. TLC (silica gel, CH_2Cl_2/MeOH, 90:10) R_f 0.5. λ_{max} (MeOH)/nm 260 (ε/dm^3 mol^{-1} cm^{-1} 20 700), 320 (29 500). ^{1}H NMR (DMSO-d_6, 300 MHz): δ 0.68−0.93 (m, 6H, 2 × CH_3), 1.06−1.08 (d, J = 6.9 Hz, 6H, 2 × CH_3), 1.26−1.43 (m, 4H, 2 × CH_2), 1.57−1.58 (m, 4H, 2 × CH_2), 2.84 (t, J = 6.6 Hz, 1H, CH), 3.17 (m, 1H, C5′−H), 3.39−3.41 (m, 1H, C≡CH, superimposed by H_2O), 3.47−3.57 (m, 4H, NCH_2), 3.61−3.68 (m, 1H, C5′−H), 3.92−3.94 (m, 1H, C4′−H), 4.18−4.28 (m, 2H, OCH_2), 4.33−4.37 (m, 1H, C3′−H), 4.57 (t, J = 5.4 Hz, 1H, C2′−H), 5.07 (t, J = 5.1 Hz, 1H, C5′−OH), 5.30 (d, J = 5.4 Hz, 1H, C3′−OH), 6.00 (d, J = 6.0 Hz, 1H, C1′−H), 8.36 (s, 1H, C8−H), 8.92 (s, 1H, NCH), 10.10 (s, 1H, NH). ESI-TOF m/z calcd for $C_{26}H_{39}N_7O_5$ $[M + H]^+$, 530.3085; found, 530.3080.

N^6-[(Di-*n*-butylamino)methylidene]-N^2-isobutyryl-9-[2-*O*-(propargyl)-5-*O*-(4,4′-dimethoxytrityl)-β-D-ribofuranosyl]-purin-2,6-diamine (13). Compound **12** (0.22g, 0.42 mmol) was dissolved in anhydrous pyridine (5 mL), 4,4′-dimethoxytrityl chloride (0.23 g, 0.67 mmol) was added, and the reaction mixture was stirred at rt for 12 h. After completion of the reaction (TLC monitoring), 10 mL of CH_2Cl_2 was added and the solution was washed with 5% aq $NaHCO_3$ (10 mL). The organic layer was dried over Na_2SO_4, evaporated to dryness, and coevaporated with toulene (3 × 10 mL). The residue was applied to FC (silica gel, CH_2Cl_2/acetone, 90:10) to obtain compound **13** (0.198 g, 57%) as a light yellow foam. TLC (silica gel, CH_2Cl_2/acetone, 90:10) R_f 0.3. λ_{max} (MeOH)/nm 260 (ε/dm^3 mol^{-1} cm^{-1} 27 900), 320 (30 700). ^{1}H NMR (DMSO-d_6, 300 MHz): δ 0.92 (t, 6H, J = 7.2 Hz, 2 × CH_3), 1.05 (t, J = 5.4 Hz, 6H, 2 × CH_3), 1.25−1.39 (m, 4H, 2 × CH_2), 1.55−1.61 (m, 4H, 2 × CH_2), 2.80−2.87 (m, 1H, CH), 3.16−3.19 (m, 1H, C5′−H), 3.38−3.47 (m, 3H, C≡CH, NCH_2), 3.45−3.59 (m, 2H, NCH_2), 3.70 (s, 3H, OCH_3), 3.71 (s, 3H, OCH_3), 4.04−4.06 (m, 1H, C4′-H), 4.33 (d, J = 2.4 Hz, 1H, OCH_2), 4.36 (d, J = 2.4 Hz, 1H, OCH_2), 4.52−4.58 (m, 1H, C3′−H), 4.67 (t, J = 5.1 Hz, 1H, C2′−H), 5.29 (d, J = 6.0 Hz, 1H, C3′−OH), 6.08 (d, J = 4.5 Hz, 1H, C1′−H), 6.77−6.82 (m, 4H, Ar−H), 7.16−7.26 (m, 8H, Ar−H), 7.34 (d, J = 7.2 Hz, 2H, Ar−H), 8.22 (s, 1H, C8−H), 8.93 (s, 1H, NCH), 10.07 (s, 1H, NH). ESI-TOF m/z calcd for $C_{47}H_{57}N_7O_7$ $[M + H]^+$, 832.4392; found, 832.4260.

N^6-[(Di-*n*-butylamino)methylidene]-N^2-isobutyryl-9-[2-*O*-(propargyl)-5-*O*-(4,4′-dimethoxytrityl)-β-D-ribofuranosyl]-purin-2,6-diamine 3′-(2-Cyanoethyl)-*N*,*N*-diisopropylphosphoramidite (14). To a solution of compound **13** (0.114 g, 0.15 mmol) in dry CH_2Cl_2 (10 mL) were added (i-Pr)$_2$NEt (0.035 g, 45 μL, 0.26 mmol) and 2-cyanoethyl diisopropylphosphoramidochloridite (0.048 g, 45 μL, 0.20 mmol), and the reaction mixture was stirred for 3 h at rt. After completion of the reaction (TLC monitoring), the reaction mixture was diluted with CH_2Cl_2 (30 mL), poured into 5% $NaHCO_3$ solution (20 mL), and extracted with CH_2Cl_2 (3 × 20 mL). The combined organic layers were dried over Na_2SO_4, and the solvent was evaporated. The residual foam was applied to FC (silica gel, CH_2Cl_2/acetone, 90:10). Evaporation of the main zone afforded **14** (0.108 g, 76%) as a colorless foam. TLC (silica gel, CH_2Cl_2/acetone, 90:10) R_f 0.6. ^{31}P NMR ($CDCl_3$, 121.5 MHz): 150.33, 150.76. ESI-TOF m/z calcd for $C_{56}H_{74}N_9O_8P$ $[M + H]^+$, 1032.5471; found, 1032.5447.

N^2-(Methoxyacetyl)-9-[2-*O*-(propargyl)-β-D-ribofuranosyl]-purin-2,6-diamine (15). Compound **1** (0.105 g, 0.33 mmol) was dissolved in pyridine (4 mL) at 4 °C and treated with trimethylsilyl chloride (430 μL, 3.4 mmol), and the solution was stirred for 1 h at 4 °C. The reaction mixture was diluted with MeCN (6 mL), kept at 4 °C, treated with methoxyacetyl chloride (110 μL, 1.2 mmol), and finally stirred for 40 min at 4 °C. After CH_2Cl_2 (15 mL) was added, the mixture was poured into H_2O (15 mL). The organic phase was dried over Na_2SO_4 and evaporated, and the residue was coevaporated with toluene (3 × 10 mL). The resulting foam was dissolved in MeOH/THF/28% aq NH_3 solution 1:1:1 (8 mL). After the solution stirred for 1 h at rt, the solvent was evaporated, and the remaining residue was coevaporated with toluene (3 × 10 mL) and finally subjected to FC (silica gel, CH_2Cl_2/MeOH, 93:7) to afford compound **15** (0.093 mg, 72%) as a colorless solid. TLC (silica gel, CH_2Cl_2/MeOH, 90:10) R_f 0.6. λ_{max} (MeOH)/nm 271 (ε/dm^3 mol^{-1} cm^{-1} 14 800). ^{1}H NMR (DMSO-d_6, 300 MHz): δ 3.37 (t, J = 2.4 Hz, 1H, C≡CH), 3.52−3.59 (m, 1H, C5′−H), 3.62−3.68 (m, 1H, C5′−H), 3.92−3.96 (m, 1H, C4′−H), 4.20 (br s, 2H, OCH_2), 4.25 (d, J = 2.1 Hz, 1H, OCH_2), 4.28 (d, J = 2.4 Hz, 1H, OCH_2), 4.33−4.38 (m, 1H, C3′−H), 4.58 (t, J = 5.4 Hz, 1H, C2′−H), 5.09 (t, J = 5.4 Hz, 1H, C5′−OH), 5.30 (d, J = 5.1 Hz, 1H, C3′−OH), 5.95 (d, J = 5.7 Hz, 1H, C1′−H), 7.34 (br s, 2H, 6-NH_2), 8.27 (s, 1H, C8−H), 11.58 (s, 1H, NH). ESI-TOF m/z calcd for $C_{16}H_{20}N_6O_6$ $[M + H]^+$, 393.1517; found, 393.1512.

N^6-Isobutyryl-N^2-(methoxyacetyl)-9-[2-*O*-(propargyl)-β-D-ribofuranosyl]purin-2,6-diamine (16). Compound **15** (0.165 g, 0.42 mmol) dissolved in pyridine (5 mL) at 4 °C was treated with Me_3SiCl (0.446 g, 525 μL, 4.1 mmol), and the solution stirred for 2 h at 4 °C. The reaction mixture was diluted with MeCN (8 mL), cooled to 4 °C, treated with isobutyryl chloride (0.054 g, 53 μL, 0.5 mmol), and finally stirred for 40 min at 4 °C. After CH_2Cl_2 (10 mL) was added, the reaction solution was poured into H_2O (10 mL). The organic phase was evaporated, and the residue was coevaporated with toluene (3 × 10 mL). The resulting foam was dissolved in MeOH/AcOH, 3:1 (10 mL). After 1 h at rt, the solution was evaporated, and the remaining residue was coevaporated with MeOH (3 × 10 mL) and toluene (3 × 10 mL). The resulting foam was applied to FC (silica gel, CH_2Cl_2/MeOH, 95:5) to afford compound **16** (0.100 g, 52%) as a colorless solid. TLC (silica gel, CH_2Cl_2/MeOH, 90:10) R_f 0.7. λ_{max} (MeOH)/nm 265 (ε/dm^3 mol^{-1} cm^{-1} 10 000), 286 (12 000). ^{1}H NMR (DMSO-d_6, 300 MHz): δ 1.10 (s, 3H, CH_3), 1.13 (s, 3H, CH_3), 2.99−3.08 (m, 1H, CH), 3.36 (s, 4H, C≡CH, OCH_3), 3.54−3.61 (m, 1H, C5′−H), 3.65−3.72 (m, 1H, C5′−H), 3.91−3.98 (m, 1H, C4′−H), 4.22−4.32 (m, 4H, CH_2), 4.36−4.40 (m, 1H, C3′−H), 4.63 (t, J = 5.1 Hz, 1H, C2′−H), 5.08 (t, J = 5.4 Hz, 1H, C5′−OH), 5.35 (d, J = 5.4 Hz, 1H, C3′−OH), 6.05 (d, J = 5.7 Hz, 1H, C1′−H), 8.55 (s, 1H, C8−H), 10.17 (s, 1H, NH), 11.64 (s, 1H, NH). ESI-TOF m/z calcd for $C_{20}H_{26}N_6O_7$ $[M + H]^+$, 463.1936; found, 463.1923.

N^6-Isobutyryl-N^2-(methoxyacetyl)-9-[5-*O*-(4,4′-dimethoxytrityl)-2-*O*-(propargyl)-β-D-ribofuranosyl]purin-2,6-diamine (17). To a solution of compound **16** (0.355 g, 0.77 mmol) in anhydrous pyridine (5 mL) was added 4,4′-dimethoxytrityl chloride (0.39 g, 1.16 mmol). The mixture was stirred at rt for 4 h. After completion of the reaction (TLC monitoring), 20 mL of CH_2Cl_2 was added, and the reaction mixture was poured into 5% aq $NaHCO_3$ (20 mL). The organic layer was dried over Na_2SO_4, evaporated to dryness, and coevaporated with toulene (3 × 10 mL), and the residue was applied to FC (silica gel, CH_2Cl_2/acetone, 30:20) to obtain compound **17** (0.32 g, 54%) as a colorless foam. TLC (silica gel, CH_2Cl_2/acetone, 30:20) R_f 0.6. λ_{max} (MeOH)/nm 267 (ε/dm^3 mol^{-1} cm^{-1} 14 000), 284 (15 900). ^{1}H NMR (DMSO-d_6, 300 MHz): δ 1.09 (s, 3H, CH_3), 1.12 (s, 3H, CH_3), 3.00−3.05 (m, 1H, CH), 3.15−3.18 (m, 1H, C5′−H), 3.34 (s, 3H, OCH_3, superimposed by H_2O), 3.42 (t, J = 2.4 Hz, 1H, C≡CH), 3.69, 3.70 (2s, 6H, 2 × OCH_3), 4.06−4.08 (m, 1H, C4′−H), 4.28 (s, 2H, CH_2), 4.33 (d, J = 2.1 Hz, 1H, OCH_2), 4.36 (d, J = 2.1 Hz, 1H, OCH_2), 4.53−4.56 (m, 1H, C3′−H), 4.72 (t, J = 5.1 Hz, 1H, C2′−H), 5.33 (d, J = 6.0 Hz, 1H, C1′−H), 6.10 (d, J = 4.5 Hz, 1H, C3′−OH), 6.79 (t, J = 8.7 Hz, 4H, Ar−H), 7.16−7.34 (m, 9H, Ar−H), 8.40 (s, 1H, C8−H), 10.08 (s, 1H, NH), 10.65 (s, 1H, NH). ESI-TOF m/z calcd for $C_{41}H_{44}N_6O_9$ $[M + Na]^+$, 787.3062; found, 787.3041.

dx.doi.org/10.1021/jo500392j | J. Org. Chem. 2014, 79, 4423−4437

N^6-Isobutyryl-N^2-(methoxyacetyl)-9-[5-*O*-(4,4′-dimethoxytrityl)-2-*O*-(propargyl)-β-D-ribofuranosyl]purin-2,6-diamine 3′-(2-Cyanoethyl)-*N*,*N*-diisopropylphosphoramidite (18). To a solution of compound **17** (0.26 g, 0.34 mmol) in dry CH_2Cl_2 (5 mL) were added $(i\text{-Pr})_2NEt$ (0.076 g, 100 μL, 0.59 mmol) and 2-cyanoethyl diisopropylphosphoramidochloridite (0.106 g, 100 μL, 0.46 mmol), and the reaction mixture was stirred for 4 h at rt. After completion of the reaction (TLC monitoring), the reaction mixture was diluted with CH_2Cl_2 (20 mL) and poured into 5% $NaHCO_3$ solution (25 mL). The organic layer was dried over Na_2SO_4, and the solvent was evaporated. The residual foam was applied to FC (silica gel, CH_2Cl_2/acetone, 70:30). Evaporation of the main zone afforded **18** (0.242 g, 74%) as a colorless foam. TLC (silica gel, CH_2Cl_2/acetone, 40:10) R_f 0.6. ^{31}P NMR ($CDCl_3$, 121.5 MHz): 150.55, 150.67. ESI-TOF *m*/*z* calcd for $C_{50}H_{61}N_8O_{10}P$ $[M + Na]^+$, 987.4140; found, 987.4115.

9-[2-*O*-(2-(2-Azidoethoxy)ethyl)-1*H*-1,2,3-triazol-4-yl)-methoxy)]-β-D-ribofuranosyl-purin-2,6-diamine (19). To a solution of compound **1** (0.1 g, 0.31 mmol) in H_2O/MeCN (10:1, 2 mL) was added bis-azide **4** (0.243 g, 1.56 mmol) and copper turnings, and the reaction mixture was stirred in the dark at rt overnight. After completion of the reaction (TLC monitoring), the copper turnings were filtered off, the solvent was evaporated, and the remaining residue was subjected to FC (silica gel, CH_2Cl_2/MeOH, 95:5) to obtain **19** (0.070 g, 45%) as a colorless foam. TLC (silica gel, CH_2Cl_2/MeOH, 90:10) R_f 0.9. λ_{max} (MeOH)/nm 282 (ε/dm^3 mol^{-1} cm^{-1} 10 000). ^1H NMR (DMSO-d_6, 300 MHz): δ 3.36 (m, CH_2, superimposed with D_2O), 3.56 (t, *J* = 2.4 Hz, 3H, C5′−H, CH_2), 3.60−3.65 (m, 1H, C5′−H), 3.79 (t, *J* = 5.1 Hz, 2H, CH_2), 3.94−3.96 (m, 1H, C4′−H), 4.29−4.33 (m, 1H, C3′−H), 4.46−4.56 (m, 4H, 2 × CH_2), 4.70 (d, *J* = 12.1 Hz, 1H, C2′−H), 5.25 (d, *J* = 5.1 Hz, 1H, C3′−OH), 5.41−5.45 (m, 1H, C5′−OH), 5.75 (br s, 2H, 2-NH_2), 5.85 (d, *J* = 6.6 Hz, 1H, C1′−H), 6.78 (br s, 2H, 6-NH_2), 7.87 (s, 1H, triazole-H), 7.89 (s, 1H, C8−H). ESI-TOF *m*/*z* calcd for $C_{17}H_{24}N_{12}O_5$ $[M + H]^+$, 477.2065; found, 477.2056.

Second Click Reaction of Nucleoside 1 with Monofunctionalized Nucleoside 19. To compound **1** (0.033 g, 0.10 mmol) in H_2O/MeCN (10:1, 2 mL) was added monofunctionalized nucleoside **19** (0.050 g, 0.10 mmol) and copper turnings, and the reaction mixture was stirred in the dark at rt overnight. After completion of the reaction (TLC monitoring), the copper turnings were filtered off, the solvent was evaporated, and the residue was coevaporated with methanol (2 × 2 mL). The residue was further washed successively with methanol (2 mL) and dichloromethane (2 mL) and dried under reduced pressure to obtain **20** (0.075 g, 60%) as a colorless solid. The analytical data are identical to compound **20** as given below.

Bis[({1,1′-(oxybis(ethane-2,1-diyl)methylene)}-1*H*-1,2,3-triazole-4,1-diyl)]-9-(β-D-ribofuranosyl)purin-2,6-diamine (20). To compound **1** (0.10 g, 0.30 mmol) in H_2O/MeCN (10:1, 2 mL) was added bis-azide **4** (0.024 g, 0.16 mmol) and copper turnings, and the reaction mixture was stirred in the dark at rt overnight. After completion of the reaction (TLC monitoring), the copper turnings were filtered, the solvent was evaporated, and the residue was coevaporated with methanol (2 × 2 mL). The residue was further washed successively with methanol (2 mL) and dichloromethane (2 mL) and dried under reduced pressure to obtain **20** (0.035 g, 42%) as a colorless solid. TLC (silica gel, CH_2Cl_2/MeOH, 80:20) R_f 0.1. λ_{max} (MeOH)/nm 282 (ε/dm^3 mol^{-1} cm^{-1} 27 700). ^1H NMR (DMSO-d_6, 300 MHz): δ 3.17 (d, 1H, *J* = 4.8 Hz, CH_2), 3.56−3.62 (m, 4H, 2 × C5′−H), 3.69−3.72 (m, 4H, 2 × CH_2), 3.95 (br s, 2H, 2 × C4′−H), 4.33−4.36 (m, 2H, 2 × C3′−H), 4.41−4.44 (m, 4H, 2 × CH_2), 4.50−4.54 (m, 4H, 2 × CH_2), 4.67 (m, 2H, 2 × C2′−H), 5.28 (d, *J* = 5.1 Hz, 2H, 2 × C3′−OH), 5.41−5.45 (m, 2H, 2 × C5′−OH), 5.78 (br s, 4H, 2 × 2-NH_2), 5.85 (d, *J* = 6.3 Hz, 2H, 2 × C1′−H), 6.81 (br s, 4H, 2 × 6-NH_2), 7.77 (s, 2H, 2 × triazole-H), 7.87 (s, 2H, 2 × C8−H). ESI-TOF *m*/*z* calcd for $C_{30}H_{40}N_{18}O_9$ $[M + Na]^+$, 819.3118; found, 819.3116.

General Procedure for the Synthesis of Azido-Modified Oligonucleotides by the Stepwise Click Functionalization Using Bis-azide 4 ("First Click"). To the single-stranded oligonucleotide **38** (3.0 A_{260} units, 30 μmol) in a H_2O/CH_3CN mixture (10:1, 100 μL) was added bis-azide **4** (37.5 μL of a 20 mmol stock solution in THF/H_2O, 1:1). After copper turnings were added, the reaction mixture was stirred in the dark at room temperature for 1 h. Then, the copper turnings were removed, and the reaction was continued at room temperature for 2 h. The reaction mixture was concentrated in a SpeedVac and dissolved in 0.2 mL of bidistilled water. The reaction mixture was further purified by reversed-phase HPLC, using gradient I to give the corresponding monofunctionalized ODN **49** (2.0 A_{260} units, 70%). In a similar way, monofunctionalized oligonucleotides **50**−**58** were prepared in 60−70% yields. These monofunctionalized oligonucleotides were also prepared by the click reaction procedure as reported in the literature.[9,15]

General Procedure for the Cross-Linking of Oligonucleotides by the Stepwise Click Functionalization ("Second Click"). To the single-stranded oligonucleotide **43** (3.0 A_{260} units, 30 μmol) in a H_2O/CH_3CN mixture (10:1, 100 μL) were added 0.1 M NaCl (50 μL) and the monofunctionalized oligonucleotide **49** (3.1 A_{260} units). After copper turnings were added, the reaction mixture was stirred in the dark at room temperature for 1 h. Then, the copper turnings were removed, and the reaction was continued at room temperature for 2 h. After completion of the reaction, the reaction mixture was concentrated in a SpeedVac and dissolved in 0.2 mL of bidistilled water. The reaction mixture was further purified by reversed-phase HPLC, using gradient I to give the corresponding cross-linked **ICL-1** (1.8 A_{260} units, 55%). In a similar way, the other cross-linked oligonucleotides **ICLs 2**−**12** were prepared in 50−60% yields. These cross-linked oligonucleotides were also prepared by the click reaction procedure as reported in the literature.[9,15]

Ion-Exchange Chromatography. Ion-exchange chromatography was performed on a 4 × 250 mm DNA PA-100 column with a precolumn using an HPLC apparatus. Elution profiles were recorded at 260 nm. The alkynylated, monofunctionalized, and cross-linked oligonucleotides (0.1 A_{260} units each) were dissolved in 100 μL of water and then directly injected into the apparatus. The compounds were eluted using the following gradient: (A) 25 mM Tris-HCl, 10% MeCN, pH 7.0; (B) 25 mM Tris-HCl, 1.0 M NaCl, and 10% MeCN, pH 7.0. Elution gradient: 0−30 min 20−80% B in A with a flow rate of 0.75 mL min^{-1}.

■ ASSOCIATED CONTENT

Ⓢ Supporting Information

Coupling constants of nucleosides, structures of cross-linked and monofunctionalized oligonucleotides, HPLC purity profiles of selected oligonucleotides, melting curves of cross-linked duplexes, extinction coefficients, ^1H, ^{13}C NMR, DEPT-135 and $^1H-^{13}C$ gated-decoupled NMR spectra of the nucleoside derivatives and click conjugates. This material is available free of charge via the Internet at http://pubs.acs.org.

■ AUTHOR INFORMATION

Corresponding Author

*Phone, +49 (0) 251 53406 500; Fax, +49 (0) 251 53406 857; E-mail, frank.seela@uni-osnabrueck.de; Homepage, www.seela.net.

Notes

The authors declare no competing financial interest.

■ ACKNOWLEDGMENTS

We would like to thank Dr. S. Budow-Busse for helpful discussions and support while preparing the manuscript. We also thank Mr. H. Mei for measuring the NMR spectra and Mr. Nhat Quang Tran for the oligonucleotide syntheses. We would like to thank Dr. H. Luftmann, Organisch-Chemisches Institut, Universität Münster, Germany, for the measurement of the MALDI spectra. Financial support by ChemBiotech, Münster, Germany, is highly appreciated.

REFERENCES

(1) (a) Lee, J. B.; Campolongo, M. J.; Kahn, J. S.; Roh, Y. H.; Hartman, M. R.; Luo, D. *Nanoscale* **2010**, *2*, 188−197. (b) Maiti, P. K.; Pascal, T. A.; Vaidehi, N.; Goddard, W. A. *J. Nanosci. Nanotechnol.* **2007**, *7*, 1712−1720. (c) Mahenthiralingam, E.; Bischof, J.; Byrne, S. K.; Radomski, C.; Davies, J. E.; Av-Gay, Y.; Vandamme, P. *J. Clin. Microbiol.* **2000**, *38*, 3165−3173. (d) Kwon, Y.-W.; Lee, C. H.; Choi, D.-H.; Jin, J.-I. *J. Mater. Chem.* **2009**, *19*, 1353−1380.

(2) (a) Yan, H.; Zhang, X.; Shen, Z.; Seeman, N. C. *Nature* **2002**, *415*, 62−65. (b) Niemeyer, C. M.; Adler, M. *Angew. Chem., Int. Ed.* **2002**, *41*, 3779−3783. (c) Müller, B. K.; Reuter, A.; Simmel, F. C.; Lamb, D. C. *Nano Lett.* **2006**, *6*, 2814−2820. (d) Shin, J.-S.; Pierce, N. A. *J. Am. Chem. Soc.* **2004**, *126*, 10834−10835. (e) Wilner, O. I.; Willner, I. *Chem. Rev.* **2012**, *112*, 2528−2556.

(3) (a) Eckstein, F. *Antisense Nucleic Acid Drug Dev.* **2000**, *10*, 117−121. (b) Heasman, J. *Dev. Biol.* **2002**, *243*, 209−214. (c) Kurreck, J. *Eur. J. Biochem.* **2003**, *270*, 1628−1644. (d) Baker, B. F.; Lot, S. S.; Condon, T. P.; Cheng-Flournoy, S.; Lesnik, E. A.; Sasmor, H. M.; Bennett, C. F. *J. Biol. Chem.* **1997**, *272*, 11994−12000. (e) Monia, B. P.; Lesnik, E. A.; Gonzalez, C.; Lima, W. F.; McGee, D.; Guinosso, C. J.; Kawasaki, A. M.; Cook, P. D.; Freier, S. M. *J. Biol. Chem.* **1993**, *268*, 14514−14522. (f) Nielsen, P. E. *Methods Enzymol.* **2000**, *313*, 156−164. (g) Orum, H.; Wengel, J. *Curr. Opin. Mol. Ther.* **2001**, *3*, 239−243.

(4) (a) Zamecnik, P. C.; Stephenson, M. L. *Proc. Natl. Acad. Sci. U.S.A.* **1978**, *75*, 280−284. (b) Stephenson, M. L.; Zamecnik, P. C. *Proc. Natl. Acad. Sci. U.S.A.* **1978**, *75*, 285−288. (c) Manoharan, M. *Antisense Nucleic Acid Drug. Dev.* **2002**, *12*, 103−128. (d) Aboul-Fadl, T. *Curr. Med. Chem.* **2005**, *12*, 2193−2214.

(5) Hofr, C.; Brabec, V. *Biopolymers* **2005**, *77*, 222−229.

(6) (a) Mei, H.; Röhl, I.; Seela, F. *J. Org. Chem.* **2013**, *78*, 9457−9463. (b) Miyake, Y.; Togashi, H.; Tashiro, M.; Yamaguchi, H.; Oda, S.; Kudo, M.; Tanaka, Y.; Kondo, Y.; Sawa, R.; Fujimoto, T.; Machinami, T.; Ono, A. *J. Am. Chem. Soc.* **2006**, *128*, 2172−2173. (c) Kuklenyik, Z.; Marzilli, L. G. *Inorg. Chem.* **1996**, *35*, 5654−5662. (d) Ono, A.; Cao, S.; Togashi, H.; Tashiro, M.; Fujimoto, T.; Machinami, T.; Oda, S.; Miyake, Y.; Okamoto, I.; Tanaka, Y. *Chem. Commun.* **2008**, 4825−4827.

(7) (a) Huisgen, R.; Szeimies, G.; Möbius, L. *Chem. Ber.* **1967**, *100*, 2494−2507. (b) Tornøe, C. W.; Christensen, C.; Meldal, M. *J. Org. Chem.* **2002**, *67*, 3057−3064. (c) Rostovtsev, V. V.; Green, L. G.; Fokin, V. V.; Sharpless, K. B. *Angew. Chem., Int. Ed.* **2002**, *41*, 2596−2599. (d) Meldal, M.; Tornøe, C. W. *Chem. Rev.* **2008**, *108*, 2952−3015. (e) Fischler, M.; Sologubenko, A.; Mayer, J.; Clever, G.; Burley, G.; Gierlich, J.; Carell, T.; Simon, U. *Chem. Commun.* **2008**, 169−171. (f) Seela, F.; Pujari, S. S. *Bioconjugate Chem.* **2010**, *21*, 1629−1641.

(8) (a) Pujari, S. S.; Xiong, H.; Seela, F. *J. Org. Chem.* **2010**, *75*, 8693−8696. (b) Xiong, H.; Seela, F. *J. Org. Chem.* **2011**, *76*, 5584−5597. (c) Pujari, S. S.; Seela, F. *J. Org. Chem.* **2012**, *77*, 4460−4465.

(9) Pujari, S. S.; Seela, F. *J. Org. Chem.* **2013**, *78*, 8545−8561.

(10) (a) Howard, F. B.; Frazier, J.; Singer, M. F.; Miles, H. T. *J. Mol. Biol.* **1966**, *16*, 415−439. (b) Howard, F. B.; Miles, H. T. *Biochemistry* **1984**, *23*, 6723−6732.

(11) Seela, F.; Becher, G. *Nucleic Acids Res.* **2001**, *29*, 2069−2078.

(12) Thomas, J. R.; Liu, X.; Hergenrother, P. J. *J. Am. Chem. Soc.* **2005**, *127*, 12434−12435.

(13) (a) Beigelman, L.; Haeberli, P.; Sweedler, D.; Karpeisky, A. *Tetrahedron* **2000**, *56*, 1047−1056. (b) Jawalekar, A. M.; Op de Beeck, M.; van Delft, F. L.; Madder, A. *Chem. Commun.* **2011**, *47*, 2796−2798.

(14) (a) Luyten, I.; Van Aerschot, A.; Rozenski, J.; Busson, R.; Herdewijn, P. *Nucleosides, Nucleotides Nucleic Acids* **1997**, *16*, 1649−1652. (b) Matray, T.; Gamsey, S.; Pongracz, K.; Gryaznov, S. *Nucleosides, Nucleotides Nucleic Acids* **2000**, *19*, 1553−1567. (c) Porcher, S.; Pitsch, S. *Helv. Chim. Acta* **2005**, *88*, 2683−2704. (d) Pasternak, A.; Kierzek, E.; Pasternak, K.; Turner, D. H.; Kierzek, R. *Nucleic Acids Res.* **2007**, *35*, 4055−4063. (e) Brown, T.; Booth, E. D.; Craig, A. G. *Nucleosides, Nucleotides Nucleic Acids* **1989**, *8*, 1051. (f) Gaffney, B. L.; Marky, L. A.; Jones, R. A. *Tetrahedron* **1984**, *40*, 3−13. (g) Okamoto, A.; Tanaka, K.; Saito, I. *Bioorg. Med. Chem. Lett.* **2002**, *12*, 97−99.

(15) Xiong, H.; Seela, F. *Bioconjugate Chem.* **2012**, *23*, 1230−1243.

(16) (a) Srivastava, S. C.; Raza, S. K. Propargyl Modified Nucleosides and Nucleotides, Patent No. US005744595A, 1998. (b) Jawalekar, A. M.; Meeuwenoord, N.; Cremers, J.; (Sjef), G. O.; Overkleeft, H. S.; van der Marel, G. A.; Rutjes, F. P. J. T.; van Delft, F. L. *J. Org. Chem.* **2008**, *73*, 287−290. (c) Anisuzzaman, A. K. M.; Alam, F.; Soloway, A. H. *Polyhedron* **1990**, *9*, 891−892. (d) Zatsepin, T. S.; Romanova, E. A.; Oretskaya, T. S. *Russ. Chem. Rev.* **2002**, *71*, 513−534. (e) Wojtczak, B. A.; Andrysiak, A.; Grüner, B.; Lesnikowski, Z. J. *Chem.—Eur. J.* **2008**, *14*, 10675−10682.

(17) (a) Egli, M.; Minasov, G.; Tereshko, V.; Pallan, P. S.; Teplova, M.; Inamati, G. B.; Lesnik, E. A.; Owens, S. R.; Ross, B. S.; Prakash, T. P.; Manoharan, M. *Biochemistry* **2005**, *44*, 9045−9057. (b) Yamada, T.; Peng, C. G.; Matsuda, S.; Addepalli, H.; Jayaprakash, K. N.; Alam, Md. R.; Mills, K.; Maier, M. A.; Charisse, K.; Sekine, M.; Manoharan, M.; Rajeev, K. G. *J. Org. Chem.* **2011**, *76*, 1198−1211.

(18) Seela, F.; Kaiser, K. *Nucleic Acids Res.* **1987**, *15*, 3113−3129.

(19) (a) Grøtli, M.; Douglas, M.; Eritja, R.; Sproat, B. S. *Tetrahedron* **1998**, *54*, 5899−5914. (b) Froehler, B. C.; Jones, R. J.; Cao, X.; Terhorst, T. J. *Tetrahedron Lett.* **1993**, *34*, 1003−1006. (c) Lesnik, E. A.; Guinosso, C. J.; Kawasaki, A. M.; Sasmor, H.; Zounes, M.; Cummins, L. L.; Ecker, D. J.; Cook, P. D.; Freier, S. M. *Biochemistry* **1993**, *32*, 7832−7838. (d) Sproat, B. S.; Iribarren, A. M.; Garcia, R. G.; Beijer, B. *Nucleic Acids Res.* **1991**, *19*, 733−738.

(20) (a) Howard, F. B.; Frazier, J.; Miles, H. T. *Biochemistry* **1976**, *15*, 3783−3795. (b) Scheit, K. H.; Rackwitz, H.-R. *Nucleic Acids Res.* **1982**, *10*, 4059−4069.

(21) Cheong, C.; Tinoco, I., Jr.; Chollet, A. *Nucleic Acids Res.* **1988**, *16*, 5115−5122.

(22) Schneider, B.; Ginell, S. L.; Jones, R.; Gaffney, B.; Berman, H. M. *Biochemistry* **1992**, *31*, 9622−9628.

(23) Ohkubo, A.; Kasuya, R.; Sakamoto, K.; Miyata, K.; Taguchi, H.; Nagasawa, H.; Tsukahara, T.; Watanobe, T.; Maki, Y.; Seio, K.; Sekine, M. *Nucleic Acids Res.* **2008**, *36*, 1952−1964.

(24) (a) Kumar, R.; El-Sagheer, A.; Tumpane, J.; Lincoln, P.; Wilhelmsson, L. M.; Brown, T. *J. Am. Chem. Soc.* **2007**, *129*, 6859−6864. (b) Wirges, C. T.; Gramlich, P. M. E.; Gutsmiedl, K.; Gierlich, J.; Burley, G. A.; Carell, T. *QSAR Comb. Sci.* **2007**, *26*, 1159−1164.

(25) Ingale, S. A.; Seela, F. *J. Org. Chem.* **2013**, *78*, 3394−3399.

(26) (a) Alefelder, S.; Sigurdsson, S. Th. *Bioorg. Med. Chem.* **2000**, *8*, 269−273. (b) Ye, M.; Guillaume, J.; Liu, Y.; Sha, R.; Wang, R.; Seeman, N. C.; Canary, J. W. *Chem. Sci.* **2013**, *4*, 1319−1329. (c) Noronha, A. M.; Noll, D. M.; Wilds, C. J.; Miller, P. S. *Biochemistry* **2002**, *41*, 760−771. (d) Ferentz, A. E.; Keating, T. A.; Verdine, G. L. *J. Am. Chem. Soc.* **1993**, *115*, 9006−9014. (e) Angelov, T.; Guainazzi, A.; Schärer, O. D. *Org. Lett.* **2009**, *11*, 661−664. (f) Weller, R. L.; Rajski, S. R. *Org. Lett.* **2005**, *7*, 2141−2144. (g) Kiviniemi, A.; Virta, P.; Drenichev, M. S.; Michailov, S. N.; Lönnberg, H. *Bioconjugate Chem.* **2011**, *22*, 1249−1255.

(27) Robins, M. J.; Zou, R.; Hansske, F.; Wnuk, S. F. *Can. J. Chem.* **1997**, *75*, 762−767.